

## A Novel Strategy for Realizing Dual State Fluorescence and Low-Temperature Phosphorescence

Yunxiang Lei<sup>a</sup>, Wenbo Dai<sup>a</sup>, Zhiqi Liu<sup>a</sup>, Shuai Guo<sup>a</sup>, Zhengxu Cai<sup>\*a</sup>, Jianbing Shi<sup>a</sup>, Xiaoyan Zheng<sup>\*b</sup>, Junge Zhi<sup>b</sup>, Bin Tong<sup>a</sup> and Yuping Dong<sup>\*a</sup>

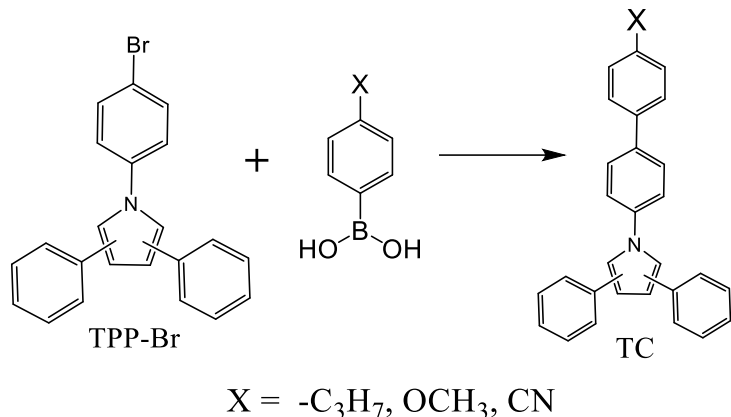
<sup>a</sup> Beijing Key Laboratory of Construction Tailorable Advanced Functional Materials and Green Applications, School of Materials Science & Engineering, Beijing Institute of Technology, 5 South Zhongguancun Street, Beijing, 100081, China

<sup>b</sup> Beijing Key Laboratory of Photoelectronic/Electrophotonic Conversion Materials, Key Laboratory of Cluster Science of Ministry of Education, School of Chemistry and Chemical Engineering, Beijing Institute of Technology, 100081 Beijing, China.

### 1. Materials and Instruments.

The target compounds were prepared by the Suzuki coupling reaction using p-cyanophenylboronic acid, p-methoxyphenylboronic acid, p-propylphenylboronic acid and **TPP-Br** isomers as raw materials with yields of 80-88%. Molecular structures of all **TPP**-based molecules were verified by Nuclear Magnetic Resonance (NMR) and Mass Spectrum (MS). The samples demonstrate good solubility in acetone, CHCl<sub>3</sub> and THF but were insoluble in water and alcohol. <sup>1</sup>H and <sup>13</sup>C NMR spectra were carried out by a Bruker ARX400 spectrometer with CDCl<sub>3</sub> as the solvent, and mass spectrum were performed by using a Finnigan BIFLEX III mass spectroscopy. UV-vis absorption spectra were measured on a Persee TU-1901 Fluorescence spectra were determined on a Hitachi F-7000 spectrophotometer. Phosphorescence spectrum were determined on a FLS920 lifetime and steady state spectrometer. X-ray crystal structure analyses were measured on Bruker-AXS SMART APEX2 CCD diffractometer. Solid-state emission quantum yields ( $\Phi_F$ ) were collected on a FluoroMax-4 (Horiba Jobin Yvon) fluorometer equipped contains an integrated sphere. All single crystals are registered on the Cambridge Crystallographic Data Centre (CCDC 1,3,4-C<sub>3</sub>H<sub>7</sub>, 1853748. 1,2,4-OCH<sub>3</sub>,

1853746. 1,3,4-OCH<sub>3</sub>, 1853750. 1,2,4-CN, 1853745. 1,2,5-CN, 1853747. 1,3,4-CN, 1853749).



Intermediate **TPP-Br** was synthesized according to literature reported methods,<sup>1-3</sup> TPP-Br (3 mmol), 4-formylbenzenboronic acid (3.2 mmol), Pd(PPh<sub>3</sub>)<sub>4</sub> (0.15 mmol), K<sub>2</sub>CO<sub>3</sub> (0.15 mmol) in 40 mL toluene and 13 ml methanol were heated under reflux for 14 h. After the reaction solution was cooled to room temperature, K<sub>2</sub>CO<sub>3</sub> and Pd(PPh<sub>3</sub>)<sub>4</sub> were filtered. After removal of solvent under reduced pressure, the crude product was purified by column chromatography (petroleum ether/ethyl acetate) to afford pure target compound.

#### **1,2,4-C<sub>3</sub>H<sub>7</sub>:**

White solid, 83.7% yield. <sup>1</sup>H NMR (CDCl<sub>3</sub>, 400 MHz). δ: 7.50-7.61 (m, 6H), 7.35-7.37 (t, 2H), 7.23-7.36 (m, 11H), 6.76 (s, 1H), 2.61-2.63 (t, 2H), 1.62-1.72 (m, 2H), 0.95-0.98 (t, 3H). <sup>13</sup>C NMR (CDCl<sub>3</sub>, 100 MHz); δ: (142.2, 134.8, 128.9, 128.7, 128.3, 127.4, 126.8, 126.6, 125.8, 125.7, 125.1, 120.8, 108.8, 37.6, 24.5, 13.8). MS (EI) m/z. 414.22 [M<sup>+</sup>].

#### **1,2,5-C<sub>3</sub>H<sub>7</sub>:**

White solid, 86.4% yield. <sup>1</sup>H NMR (CDCl<sub>3</sub>, 400 MHz). δ: 7.26-7.51 (m, 4H), 7.09-7.25 (m, 14H), 6.51(s, 2H), 2.61-2.65 (t, 2H), 1.62-1.70 (m, 2H), 0.95-0.99 (t, 3H). <sup>13</sup>C NMR (CDCl<sub>3</sub>, 100 MHz); δ: (142.2, 139.6, 137.8, 137.1, 135.8, 133.2, 129.0, 128.9, 128.7, 127.9, 126.9, 126.7, 126.2, 110.2, 37.6, 24.5, 13.8). MS (EI) m/z. 414.22 [M<sup>+</sup>].

#### **1,3,4-C<sub>3</sub>H<sub>7</sub>:**

White solid, 80.6% yield.  $^1\text{H}$  NMR ( $\text{CDCl}_3$ , 400 MHz).  $\delta$ : 7.64-7.66 (d, 2H), 7.50-7.53 (t, 4H), 7.20-7.34 (m, 14H), 2.61-2.65 (t, 2H), 1.67-1.73 (m, 2H), 0.95-0.99 (t, 3H).  $^{13}\text{C}$  NMR ( $\text{CDCl}_3$ , 100 MHz);  $\delta$ : (142.1, 139.1, 137.7, 137.4, 135.2, 129.0, 128.5, 128.2, 128.1, 126.7, 126.0, 125.7, 120.3, 118.5, 37.6, 24.5, 13.8). MS (EI) m/z. 414.22 [ $\text{M}^+$ ].

**1,2,4-OCH<sub>3</sub>:**

White solid, 88.2% yield.  $^1\text{H}$  NMR ( $\text{CDCl}_3$ , 400 MHz).  $\delta$ : 7.50-7.61 (m, 6H), 7.35-7.39 (t, 2H), 7.19-7.26 (m, 9H), 6.76-6.96 (d, 2H), 6.49 (s, 1H), 3.84 (s, 3H).  $^{13}\text{C}$  NMR ( $\text{CDCl}_3$ , 100 MHz);  $\delta$ : (159.3, 139.2, 138.9, 135.1, 134.7, 132.7, 132.5, 128.7, 128.3, 128.2, 127.9, 127.1, 126.5, 125.8, 125.6, 125.1, 120.8, 114.3, 108.8, 55.3). MS (EI) m/z. 402.18 [ $\text{M}^+$ ].

**1,2,5-OCH<sub>3</sub>:**

White solid, 87.6% yield.  $^1\text{H}$  NMR ( $\text{CDCl}_3$ , 400 MHz).  $\delta$ : 7.50-7.52 (d, 2H), 7.42-7.44 (d, 2H), 7.04-7.25 (m, 12H), 6.94-6.96 (d, 2H), 6.49 (s, 2H), 3.83 (s, 3H).  $^{13}\text{C}$  NMR ( $\text{CDCl}_3$ , 100 MHz);  $\delta$ : (159.4, 139.3, 137.5, 135.8, 133.3, 132.4, 129.1, 128.7, 128.0, 127.9, 126.7, 126.2, 114.2, 110.0, 55.3). MS (EI) m/z. 402.18 [ $\text{M}^+$ ].

**1,3,4-OCH<sub>3</sub>:**

White solid, 83.6% yield.  $^1\text{H}$  NMR ( $\text{CDCl}_3$ , 400 MHz).  $\delta$ : 7.62-7.65 (d, 2H), 7.49-7.51 (t, 4H), 7.21-7.33 (m, 12H), 7.00 (s, 2H), 3.87 (s, 3H).  $^{13}\text{C}$  NMR ( $\text{CDCl}_3$ , 100 MHz);  $\delta$ : (159.3, 138.8, 138.4, 135.3, 132.6, 128.5, 128.2, 128.0, 127.8, 126.0, 125.6, 120.3, 118.5, 114.3, 55.3). MS (EI) m/z. 402.18 [ $\text{M}^+$ ].

**1,2,4-CN:**

White solid, 84.9% yield.  $^1\text{H}$  NMR ( $\text{CDCl}_3$ , 400 MHz).  $\delta$ : 7.67-7.70 (d, 4H), 7.54-7.58 (d, 4H), 7.22-7.36 (m, 11H), 6.76 (m, 1H).  $^{13}\text{C}$  NMR ( $\text{CDCl}_3$ , 100 MHz);  $\delta$ : (132.7, 132.5, 128.7, 128.4, 128.3, 127.8, 127.5, 126.8, 126.0, 125.9, 125.1, 120.6, 111.1, 109.4). MS (EI) m/z. 397.17 [ $\text{M}^+$ ].

**1,2,5-CN:**

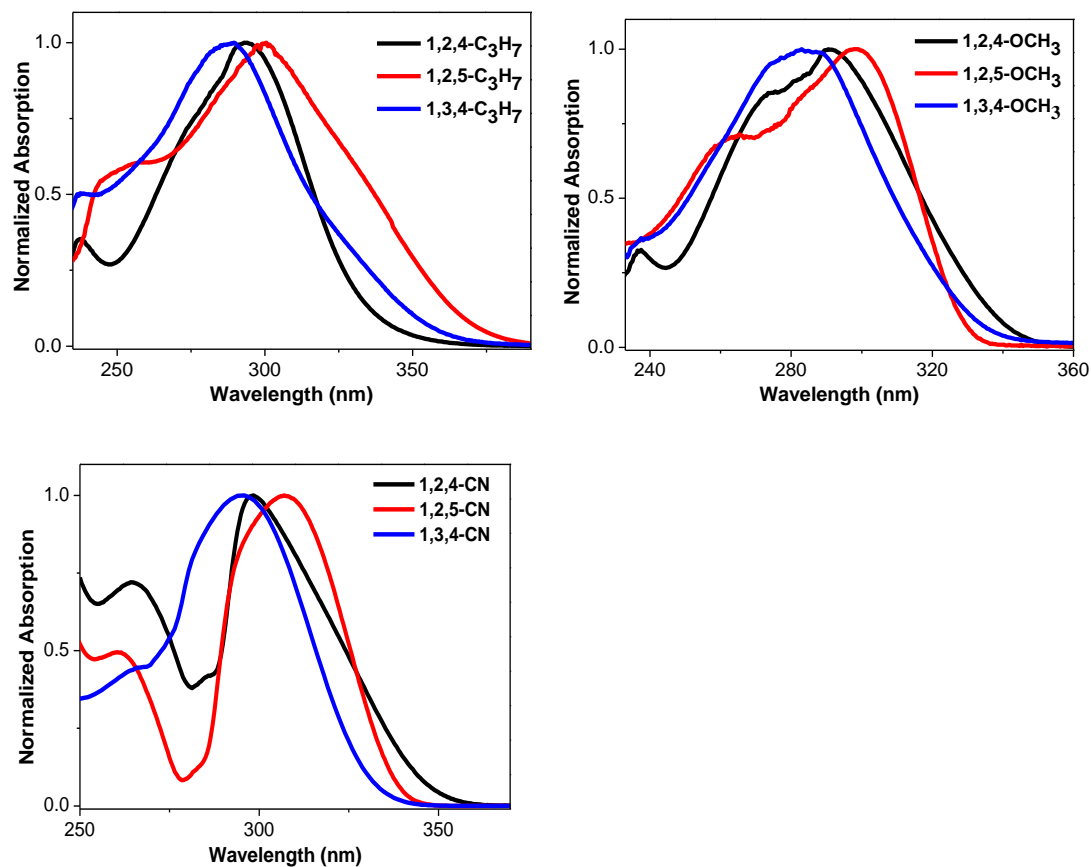
White solid, 86.7% yield.  $^1\text{H}$  NMR ( $\text{CDCl}_3$ , 400 MHz).  $\delta$ : 7.68-7.70 (d, 4H), 7.47-7.49 (d, 2H), 7.10-7.26 (m, 12H), 6.51 (m, 2H).  $^{13}\text{C}$  NMR ( $\text{CDCl}_3$ , 100 MHz);  $\delta$ : (137.5,

135.8, 133.1, 132.6, 129.4, 128.8, 127.9, 127.5, 127.4, 126.4, 111.8, 111.1, 110.4). MS (EI) m/z. 397.17 [M<sup>+</sup>].

### 1,3,4-CN:

White solid, 87.4% yield. <sup>1</sup>H NMR (CDCl<sub>3</sub>, 400 MHz). δ: 7.65-7.73 (m, 6H), 7.55-7.57 (d, 2H), 7.20-7.32 (m, 12H). <sup>13</sup>C NMR (CDCl<sub>3</sub>, 100 MHz); δ: (144.4, 140.4, 136.3, 134.9, 132.7, 128.5, 128.4, 128.2, 127.4, 126.2, 120.2, 118.8, 116.2, 111.0). MS (EI) m/z. 397.17 [M<sup>+</sup>]

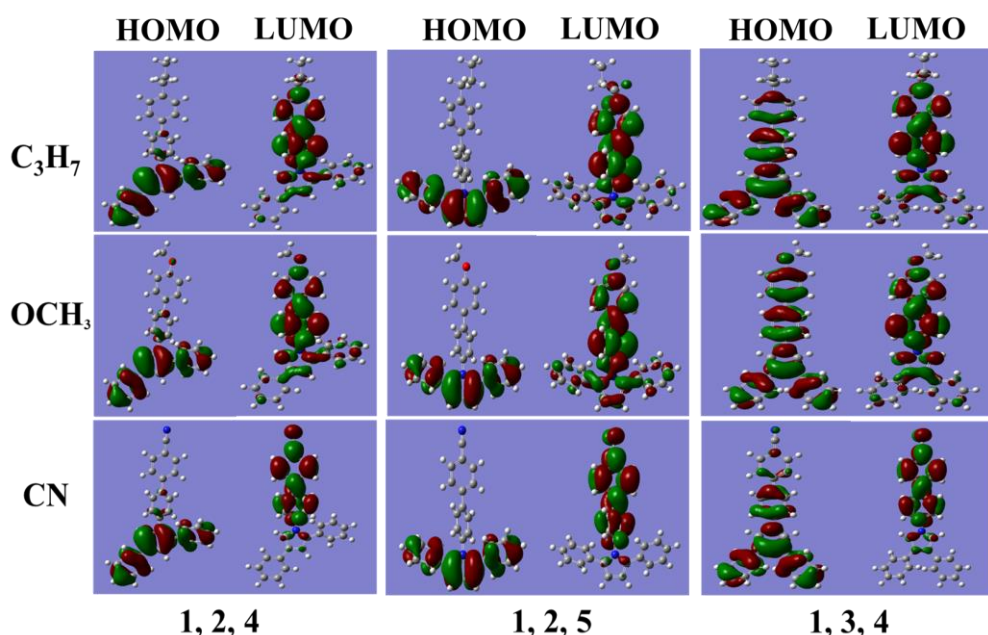
## 2. Absorption Spectra.



**Figure S1.** Absorption spectra of 10<sup>-5</sup> M THF solution of TPP-based derivatives.

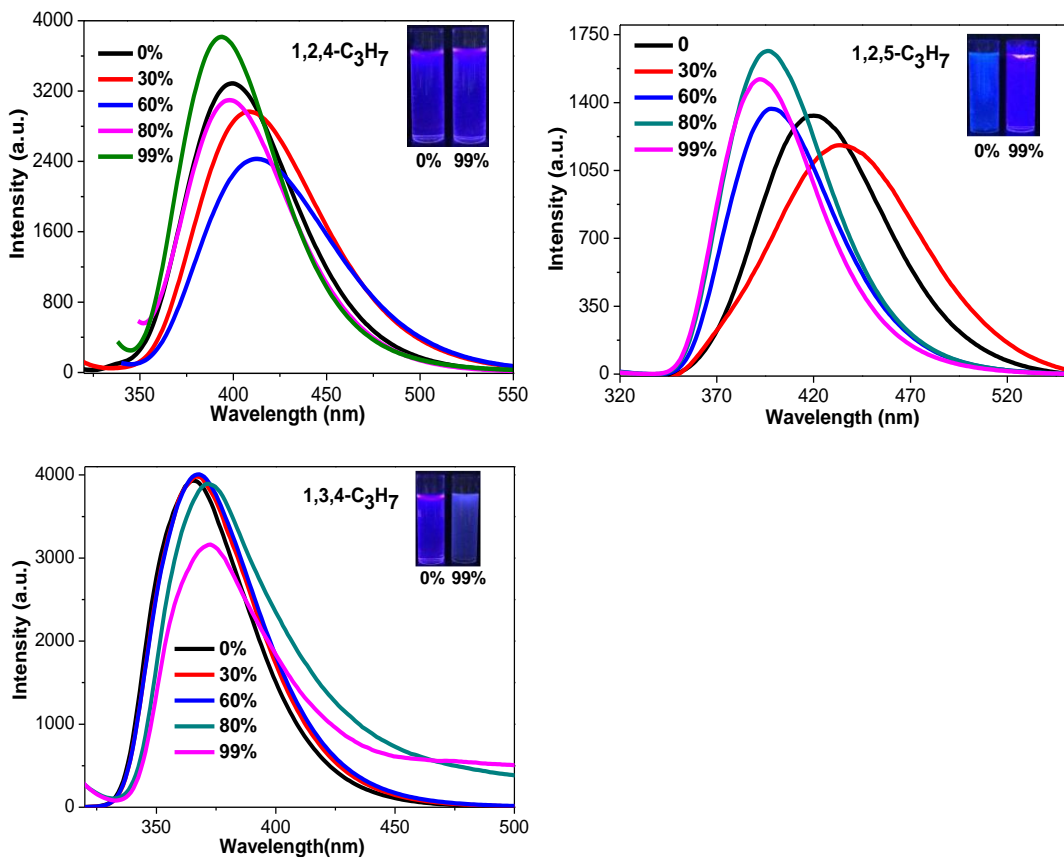
### 3. HOMO and LUMO Orbitals.

Density functional theory (DFT) calculations were performed using B3LYP/6-311+G+d method. The highest occupied molecular orbital (HOMO) and the lowest unoccupied molecular orbital (LUMO) are shown in Figure S2. The band gaps ( $E_g$ ) are listed in Table 1. Distributions of HOMO of the 1,2,4-C<sub>3</sub>H<sub>7</sub>/OCH<sub>3</sub>/CN and 1,2,5-C<sub>3</sub>H<sub>7</sub>/OCH<sub>3</sub>/CN all localized on the pyrrole moiety. The LUMO distributions of 1,2,4/1,2,5-C<sub>3</sub>H<sub>7</sub>, 1,2,4/1,2,5-OCH<sub>3</sub> are mainly localized biphenyl group and slightly localized pyrrole moiety. However, LUMO of 1,2,4/1,2,5-CN is completely distributed on the cyano- and biphenyl-group. This is caused by the push-pull electron effect existing in the D-A molecule. For the HOMO distributions of 1,3,4-C<sub>3</sub>H<sub>7</sub>/OCH<sub>3</sub>/CN samples, they are mostly located on the entire molecule due to the poorer conjugation of TPP-1,3,4 comparing to the TPP-1,2,4/1,2,5. And the distributions of LUMO for the 1,3,4-C<sub>3</sub>H<sub>7</sub>/OCH<sub>3</sub>/CN samples follow the same trend as for the 1,2,4-C<sub>3</sub>H<sub>7</sub>/OCH<sub>3</sub>/CN and 1,2,5-C<sub>3</sub>H<sub>7</sub>/OCH<sub>3</sub>/CN.

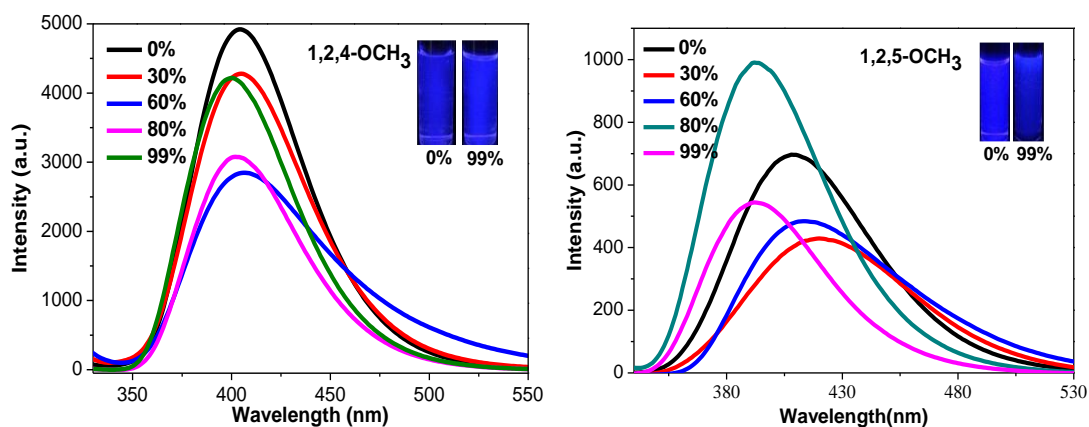


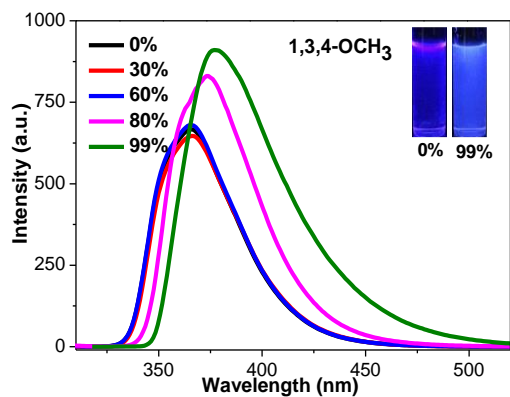
**Figure S2,** HOMO and LUMO orbitals of TPP-based compounds

#### 4. PL Spectra in THF/Water Mixtures with Different Water Volume Fractions.

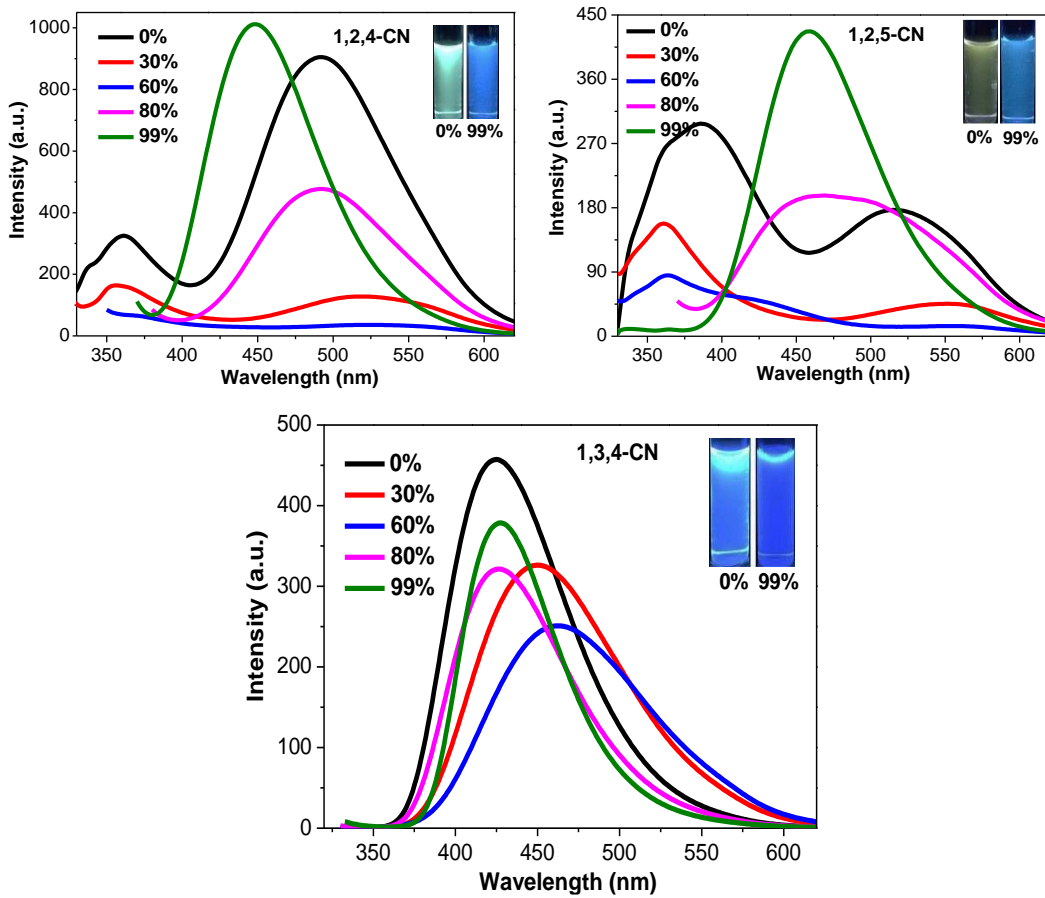


**Figure S3.** PL spectra of TPP-C<sub>3</sub>H<sub>7</sub> ( $10^{-5}$  M) in THF/water mixtures with different water volume fractions. Insets: Visible fluorescent images of TPP-based compounds with -C<sub>3</sub>H<sub>7</sub> group under a 302 nm UV lamp.

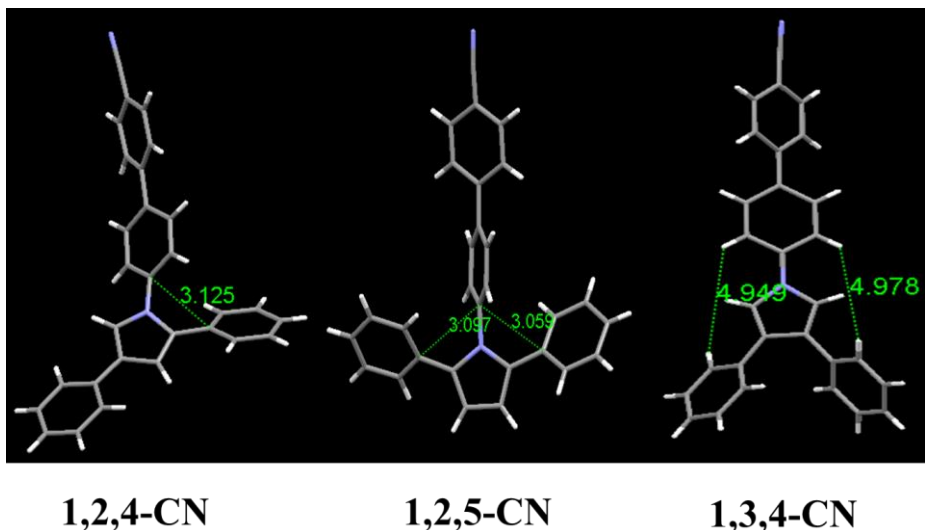




**Figure S4.** PL spectra of TPP-OCH<sub>3</sub> (10<sup>-5</sup> M) in THF/water mixtures with different water volume fractions. Insets: Visible fluorescent images of TPP-based compounds with -OCH<sub>3</sub> group under a 302 nm UV lamp.

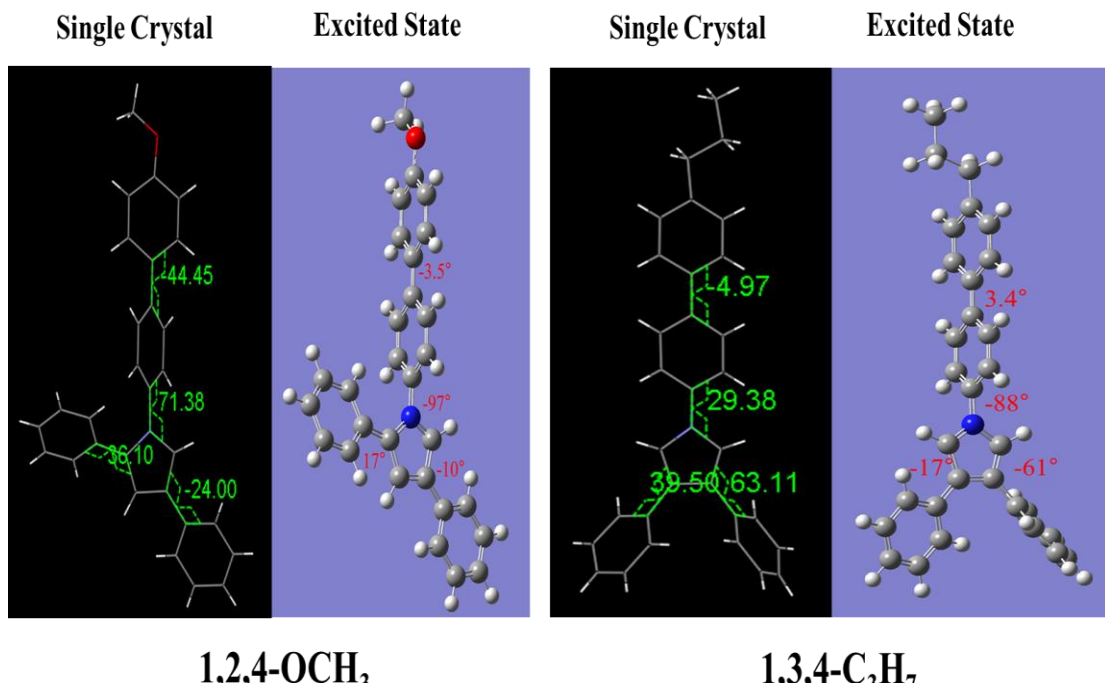


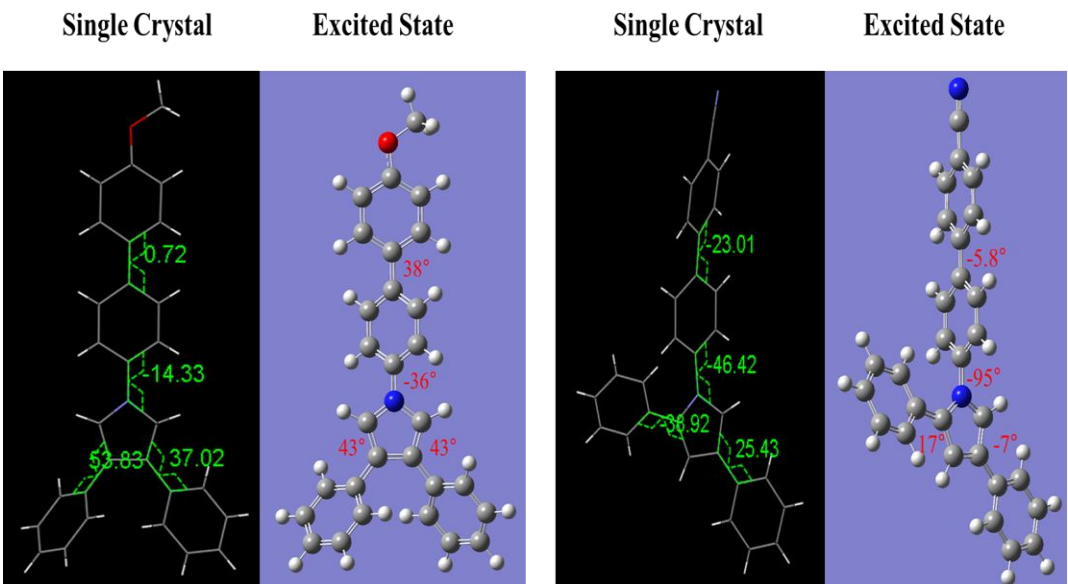
**Figure S5.** PL spectra of TPP-CN (10<sup>-5</sup> M) in THF/water mixtures with different water volume fractions. Insets: Visible fluorescent images of TPP-based compounds with -CN group under a 302 nm UV lamp.



**Figure S6.** Crystal structures of three -CN based molecules showing shortest distances between face-to-face aligned neighboring phenyl groups.

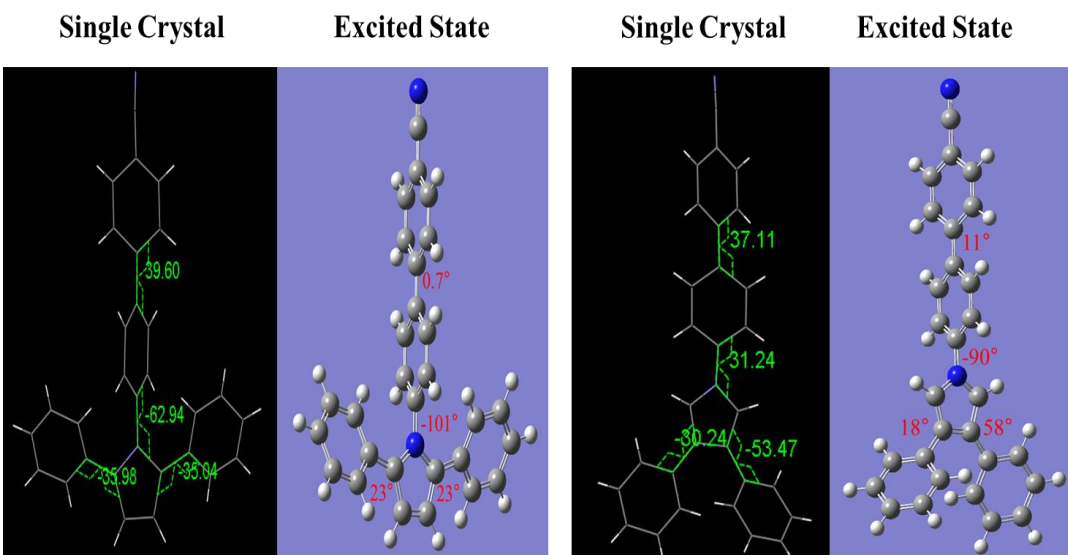
### 5. The molecule conformation of samples in ground and excited state.





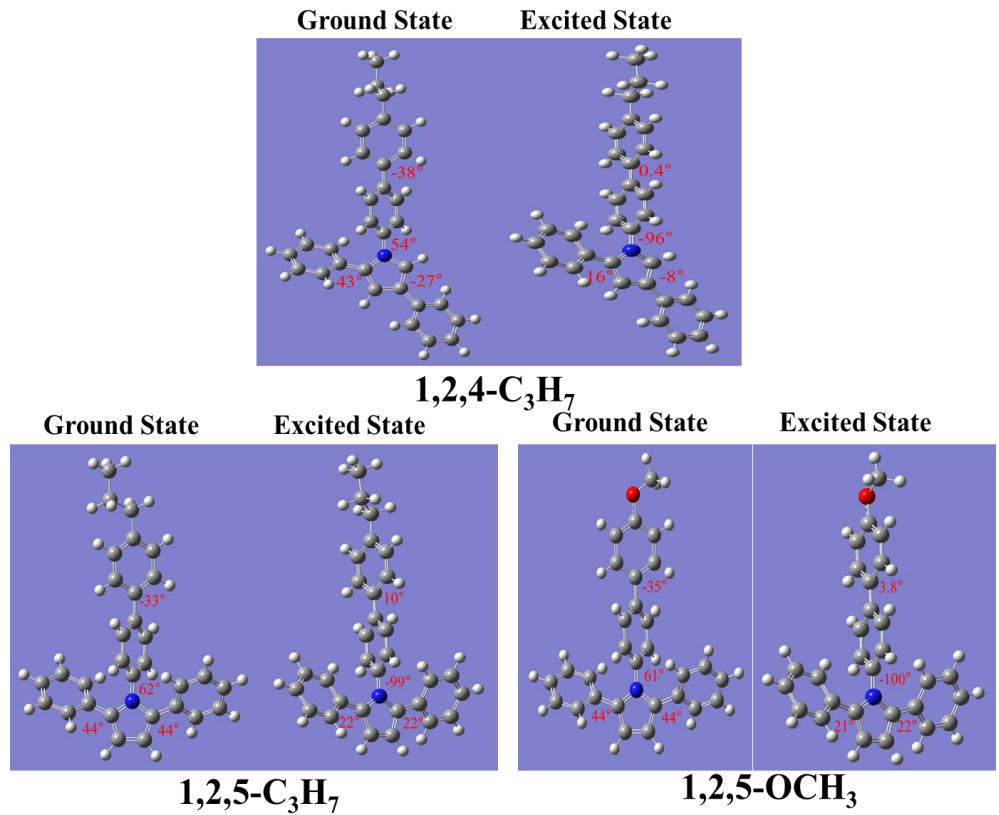
1,3,4-OCH<sub>3</sub>

1,2,4-CN



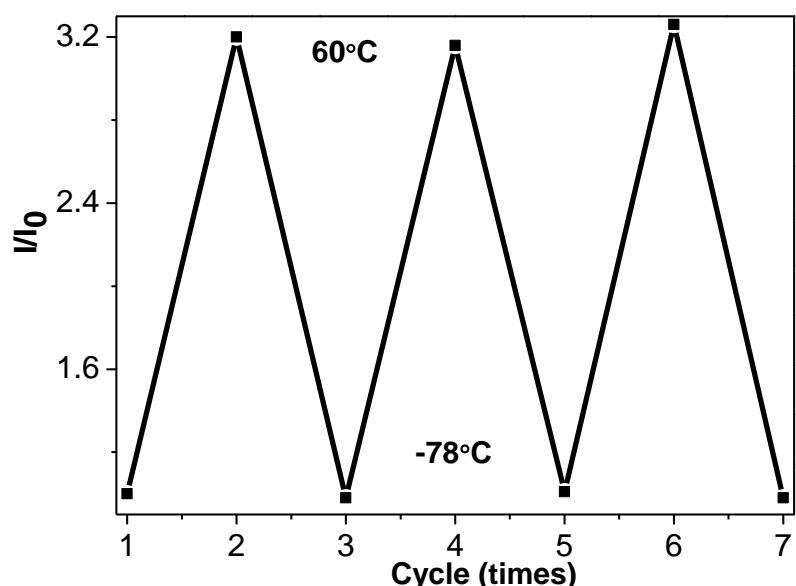
1,2,5-CN

1,3,4-CN

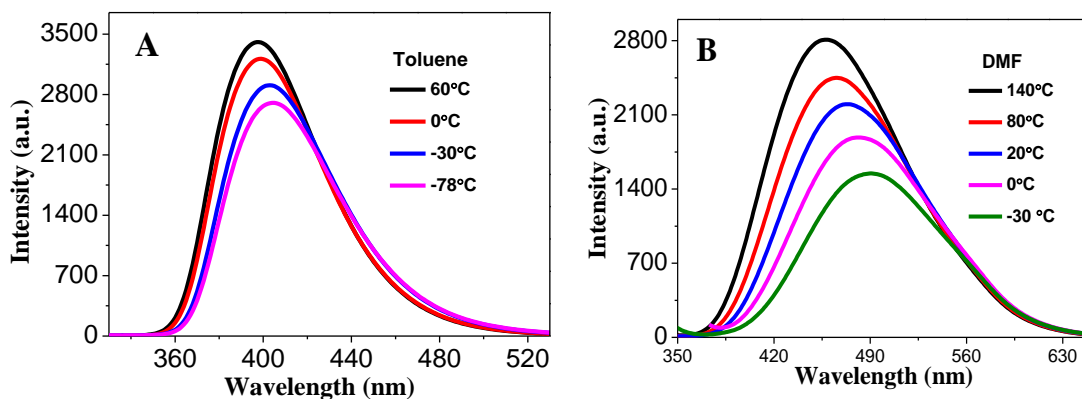


**Figure S7**, Molecular conformation of single crystal, the optimal configuration of samples in the excited state or ground state. Gray color corresponds to carbon, white to hydrogen, red to oxygen and blue to nitrogen.

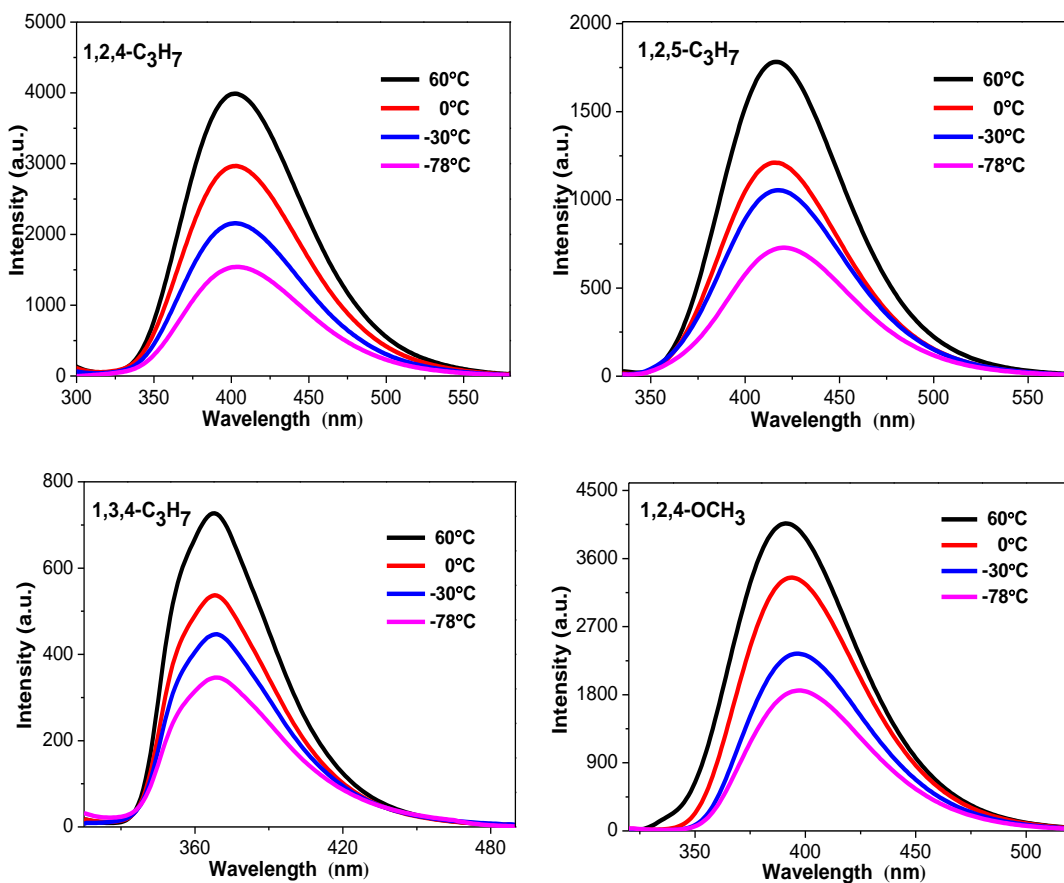
## 6. PL spectra of Samples in Different Temperature.



**Figure S8**, PL intensity of 1,3,4-CN against number of temperature.



**Figure S9.** PL spectra of 1,3,4-CN in the liquid state at different temperatures (A: toluene, B: DMF. Concentration:  $10^{-5}$  M)



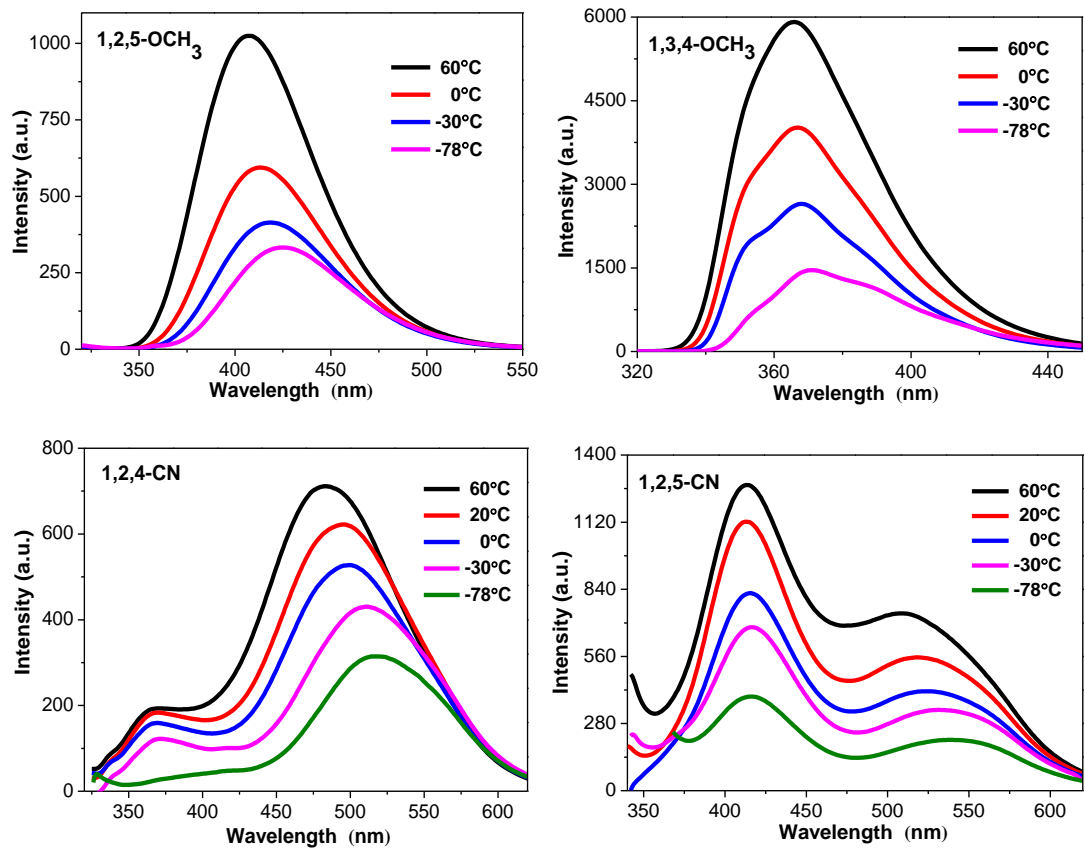


**Figure S10.** PL spectra of samples at different temperatures ( $10^{-5}$  M in THF).

### 7. PL spectra of 1,3,4-CN/OCH<sub>3</sub>/C<sub>3</sub>H<sub>7</sub> in different solvent.

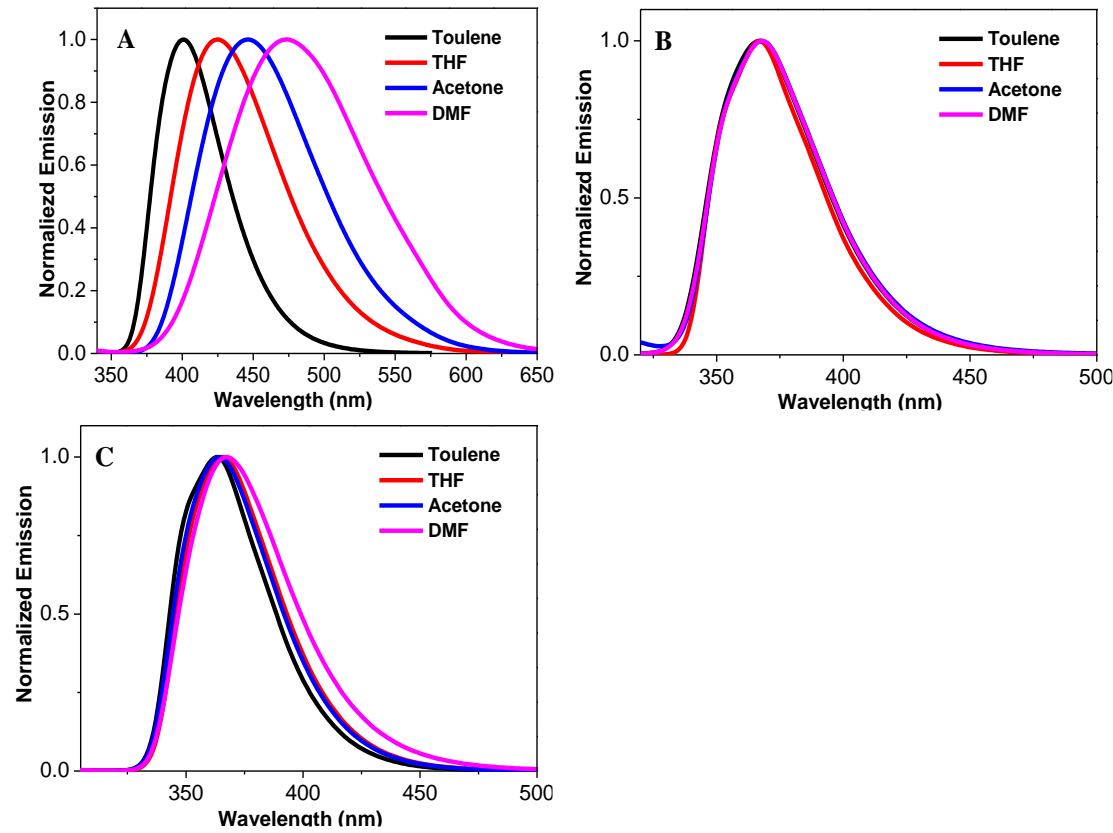


**Figure S11.** PL spectra of 1,3,4-CN(A), -OCH<sub>3</sub>(B),-C<sub>3</sub>H<sub>7</sub>(C) in different solvent ( $10^{-5}$  M).

## 8. MD Simulation.

**Table S1.** The absorption spectrum of 1,3,4-CN obtained by selected density functionals (unit: eV/nm) and the corresponding experimental results (unit: nm).

	B3LYP	CAM-B3LYP//B3LYP	PBE0	$\omega$ -B97XD	Experiment
<b>1,3,4-CN</b>	3.45/359	4.25/291	3.65/339	4.50/275	294

**Quantum calculations.** All quantum calculations were performed by Gauussion 09 software. The geometry of 134-CN was optimized by three hybrid functionals, B3LYP, PBE0<sup>1-3</sup> and  $\omega$ -B97XD<sup>4-6</sup> with basis set 6-31G(d), respectively. The obtained absorption wavelength were listed in Table 1. The maximum absorption wavelength by experiments was also included in Table 1 for comparison. With respect to the experimental result, the obtained absorption wavelength of B3LYP and PBE0 are much red-shifted, while the corresponding result of  $\omega$ -B97XD are 20 nm blue-shifted. To reproduce the experimental result, we corrected the absorption wavelength of 134-CN by CAM-B3LYP<sup>10</sup> functional based on the optimized geometry by B3LYP, referred as S<sub>0,min</sub> and we found that CAM-B3LYP can well reproduce the experimental result with only 3 nm derivation.

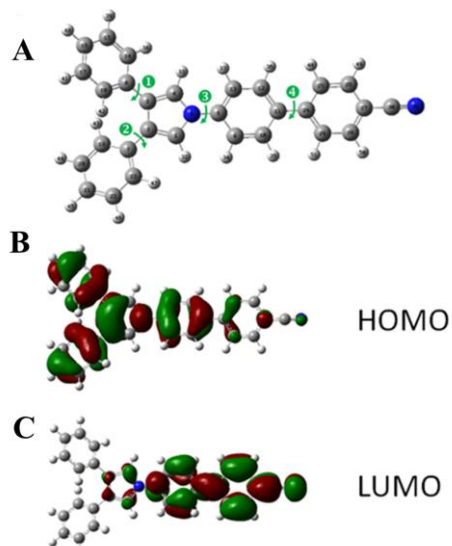


**Figure S12.** (A) The optimized geometry of 1,3,4-CN at the ground state (S0.mim) and the corresponding electron density contours of (B) HOMO and (c) LUMO.

The geometry of 1,3,4-CN at the S0 minimum and the electron density contour were

shown in Figure S12. It demonstrates that the electron density of HOMO is localized on the donor moiety while the LUMO are mainly distributed on the acceptor moiety, reflecting the DA feature of 1,3,4-CN system. For 134-CN system, the transition from HOMO to LUMO mainly take part in the electronic transition from  $S_0$  to  $S_1$ . Thus the HOMO and LUMO overlap, determined by conformation of 134-CN, play a key role in its absorption spectrum.

All MD simulations were performed using GROMACS 5.1.5 package. Atoms types and parameters of 1,3,4-CN were built from the general amber force field. The electrostatic potential of 1,3,4-CN was calculated at  $\omega$ -B97XD/6-31G6-7 level using Gaussian 09. Partial charges of atoms reproducing the electrostatic potential were obtained using restrained electrostatic potential fitting method.

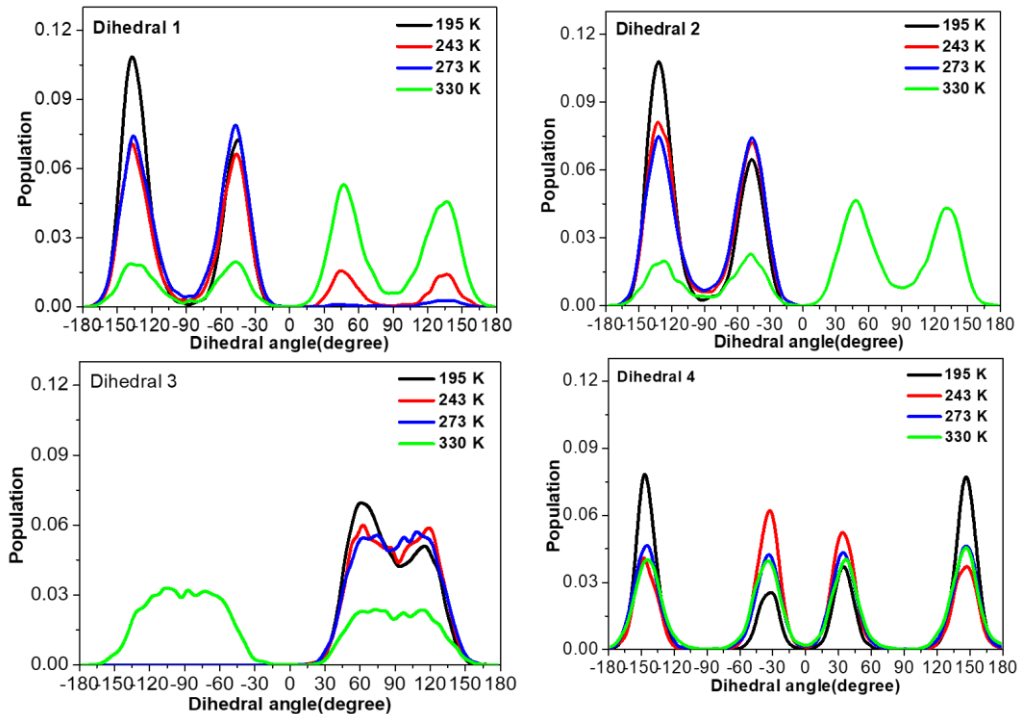


**Figure S13.** The distributions of selected dihedral angles of 1,3,4-CN system in toluene solution at four different temperatures: 195 K, 243 K, 273 K and 330 K, respectively.

## 9. References.

- [1]. P. J. Stephens, F. J. Devlin. C. F. Chabalowski, M. J. Frisch, *J. Phy. Chem.* 1994, **98**, 11623-11627.
- [2]. A. D. Becke. *J. Chem. Phy.* 1993, **98**, 5648-5652.
- [3]. M. Ernzerhof, G. E. Scuseria. *J. Chem. Phys.* 1999, **110**, 5029-5036.
- [4]. C. Adamo, V Barone. *J. Chem Phys.* 1999, **110**, 6158-6170.
- [5] J. D. Chai, H. Gordon, *Phys. Chem. Chem. Phys.* 2008, **10**, 6615-6620.
- [6] J. D.Chai, H. Gordon, M. J. *Chem Phys.* 2008, **128**, 084106.
- [7]. T. Yanai, D. P. Tew, Handy, N. C. *Chem. Phys. Lett.* 2004, **393**, 51-57.

**Table S2** The energy levels of compounds.

Sample	$\Delta E_{SG}$ (ev)	$\Delta E_{TG}$ (ev)	$\Delta E_{ST}$ (ev)
1,2,4-C <sub>3</sub> H <sub>7</sub>	4.25	3.11	1.14
1,2,5-C <sub>3</sub> H <sub>7</sub>	4.11	3.09	1.02
1,3,4-C <sub>3</sub> H <sub>7</sub>	4.34	3.18	1.16
1,2,4-OCH <sub>3</sub>	4.21	3.07	1.14
1,2,5-OCH <sub>3</sub>	4.16	3.04	1.12
1,3,4-OCH <sub>3</sub>	4.36	3.11	1.25
1,2,4-CN	3.03	2.78	0.25
1,2,5-CN	2.95	2.74	0.21
1,3,4-CN	3.26	2.95	0.31

$\Delta E_{SG}$ : The energy gap between the lowest singlet and ground state;  $\Delta E_{TG}$ : The energy gap between the lowest triplet and ground state;  $\Delta E_{ST}$ : The energy gap between the lowest singlet and triplet states.

## 10. NMR Spectra.

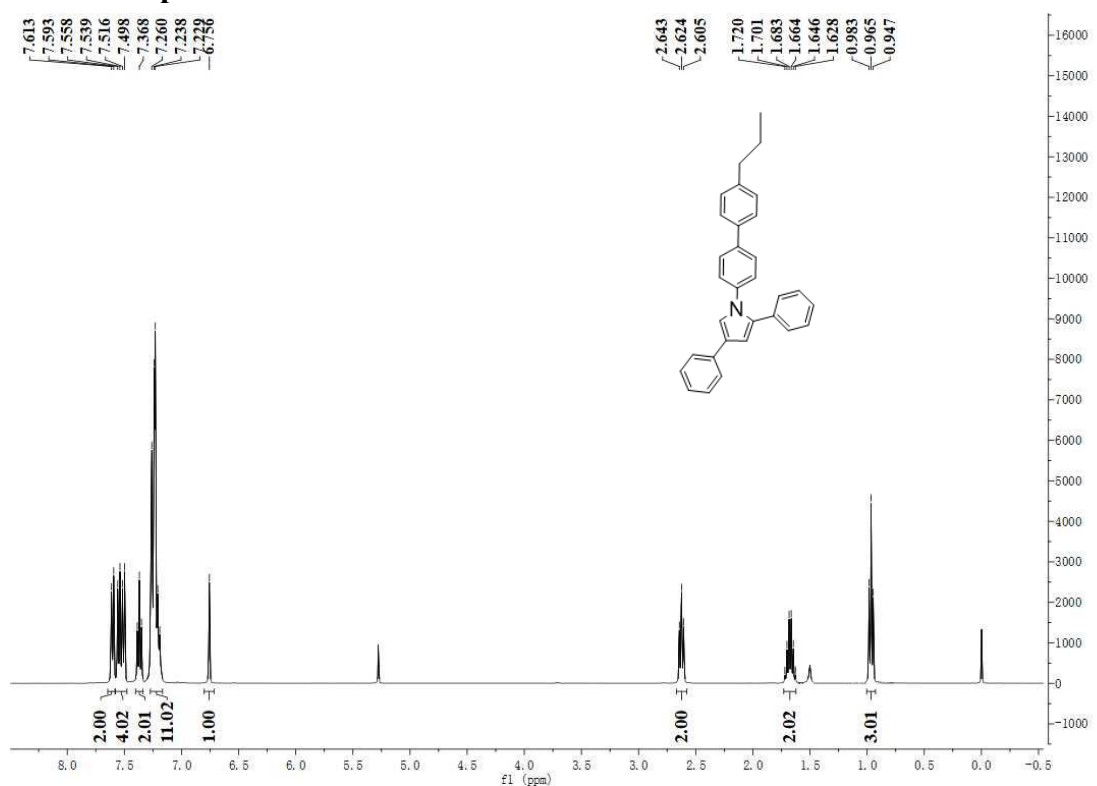


**Figure S14.** The  $^1\text{H}$  NMR of 1,2,4-C<sub>3</sub>H<sub>7</sub>. (CDCl<sub>3</sub>, 293 K, 400 M)

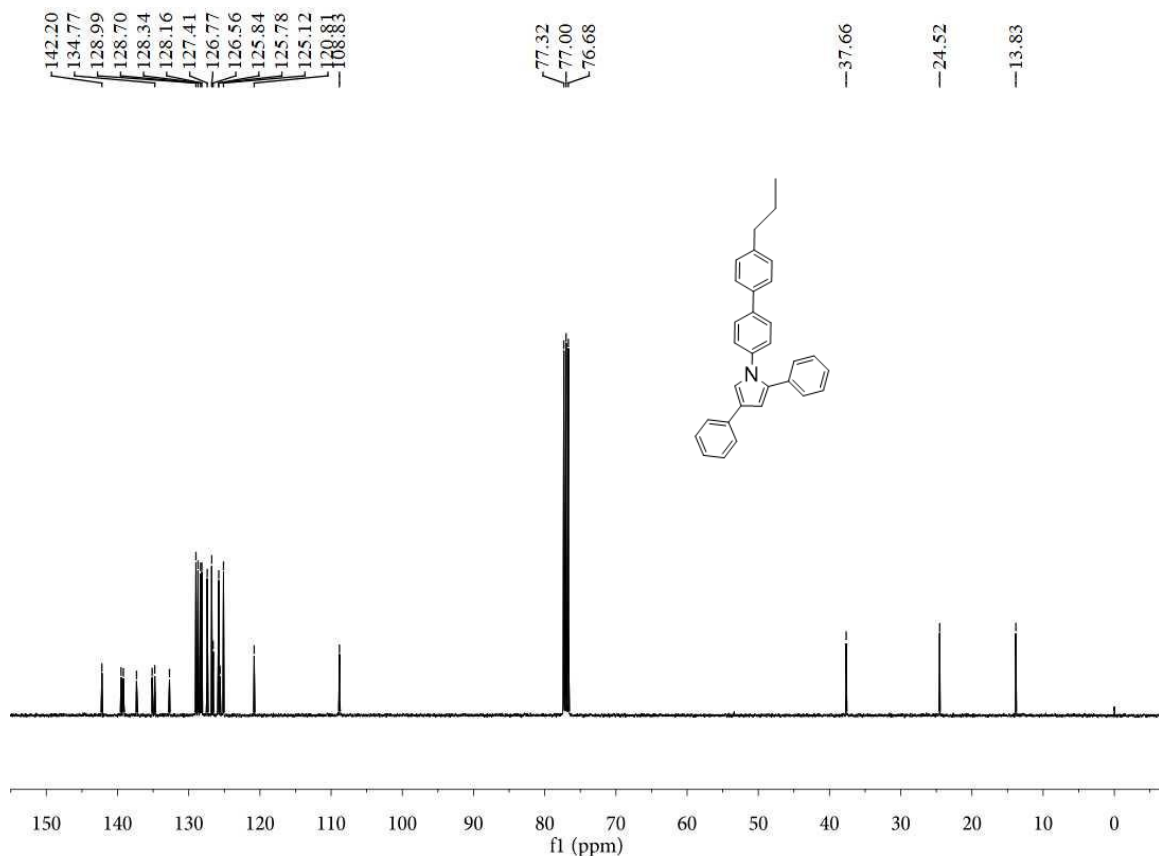


**Figure S15.** The  $^{13}\text{C}$  NMR of 1,2,4-C<sub>3</sub>H<sub>7</sub>. (CDCl<sub>3</sub>, 293 K, 400 M)

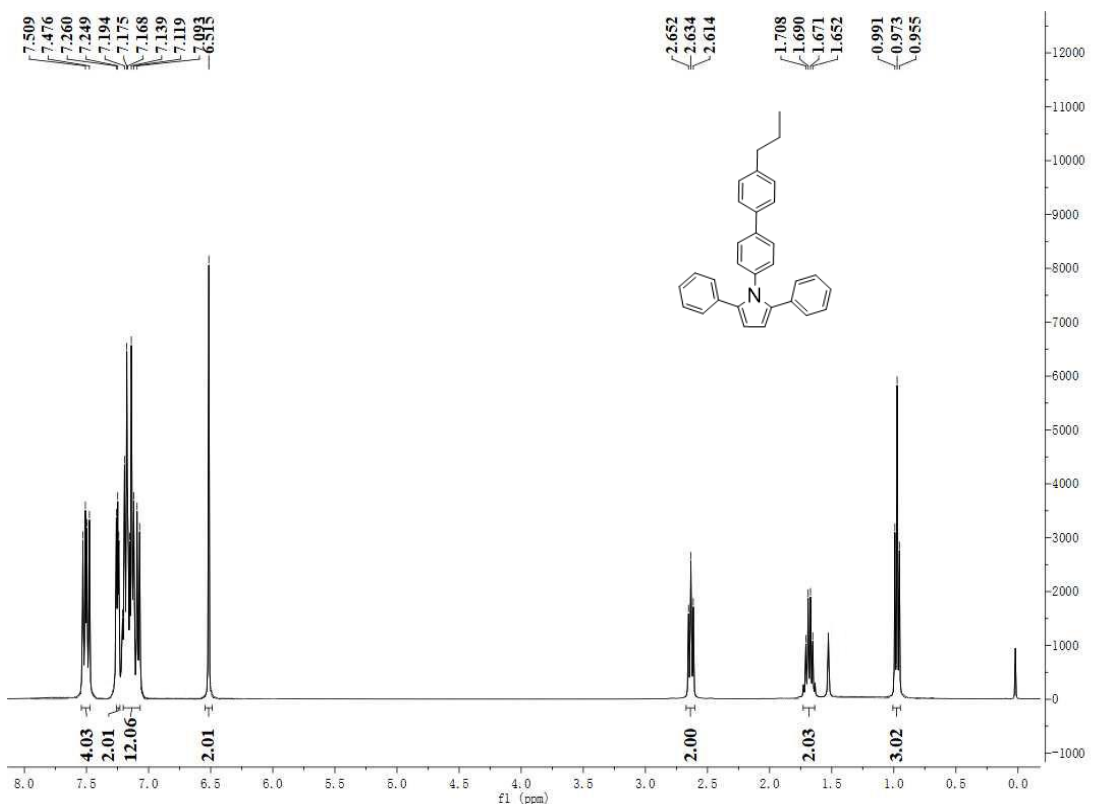


**Figure S16.** The  $^1\text{H}$  NMR of 1,2,5-C<sub>3</sub>H<sub>7</sub>. (CDCl<sub>3</sub>, 293 K, 400 M)

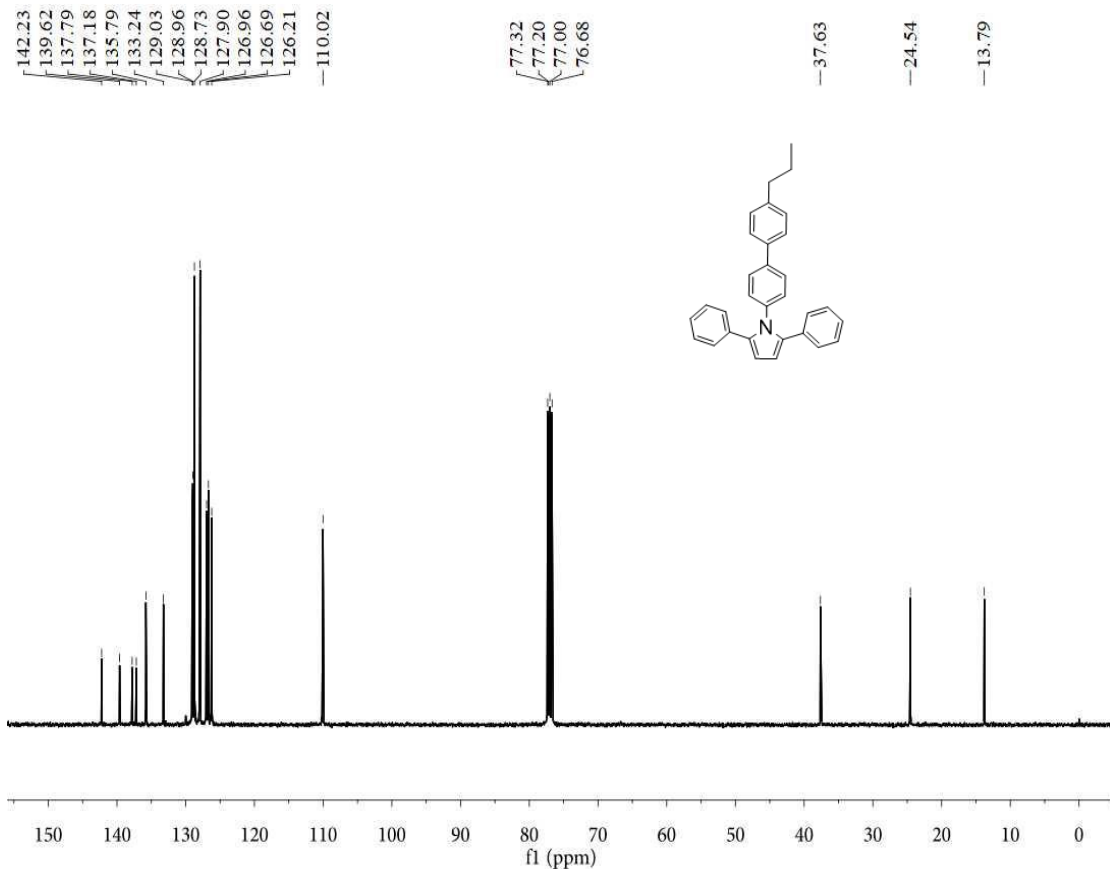


**Figure S17.** The  $^{13}\text{C}$  NMR of 1,2,5-C<sub>3</sub>H<sub>7</sub>. (CDCl<sub>3</sub>, 293 K, 400 M)

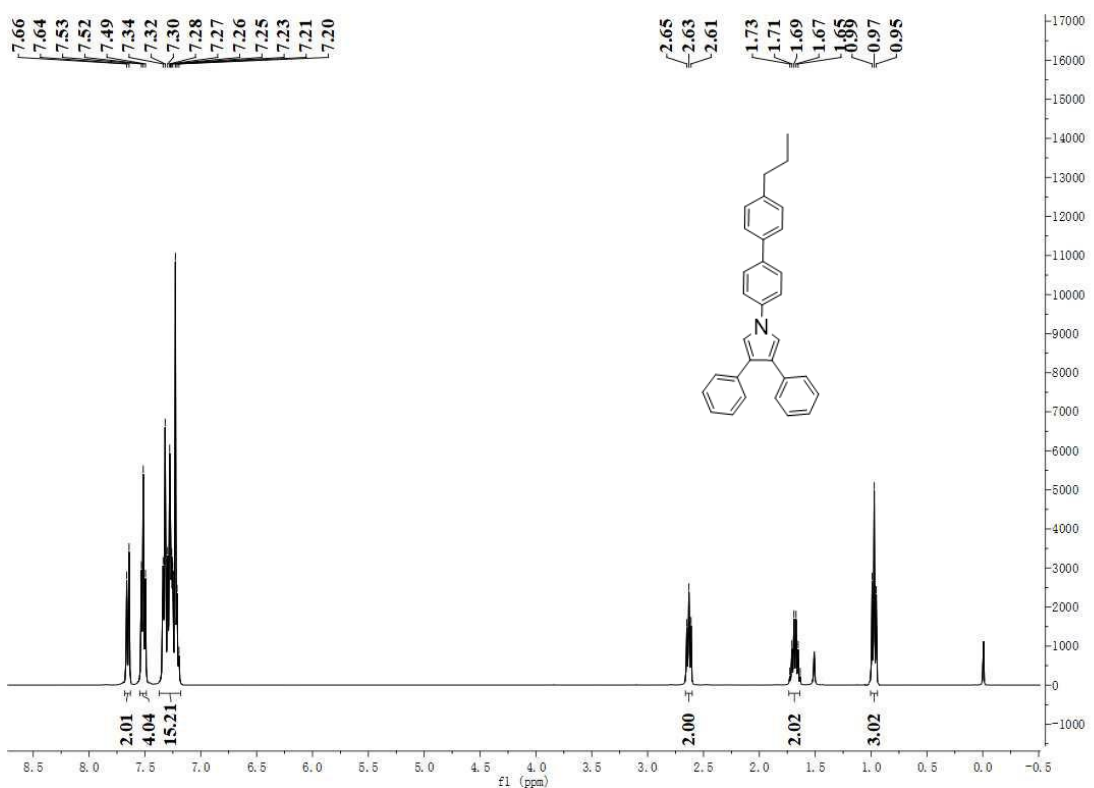


**Figure S18.** The  $^1\text{H}$  NMR of 1,3,4-C<sub>3</sub>H<sub>7</sub>. (CDCl<sub>3</sub>, 293 K, 400 M)

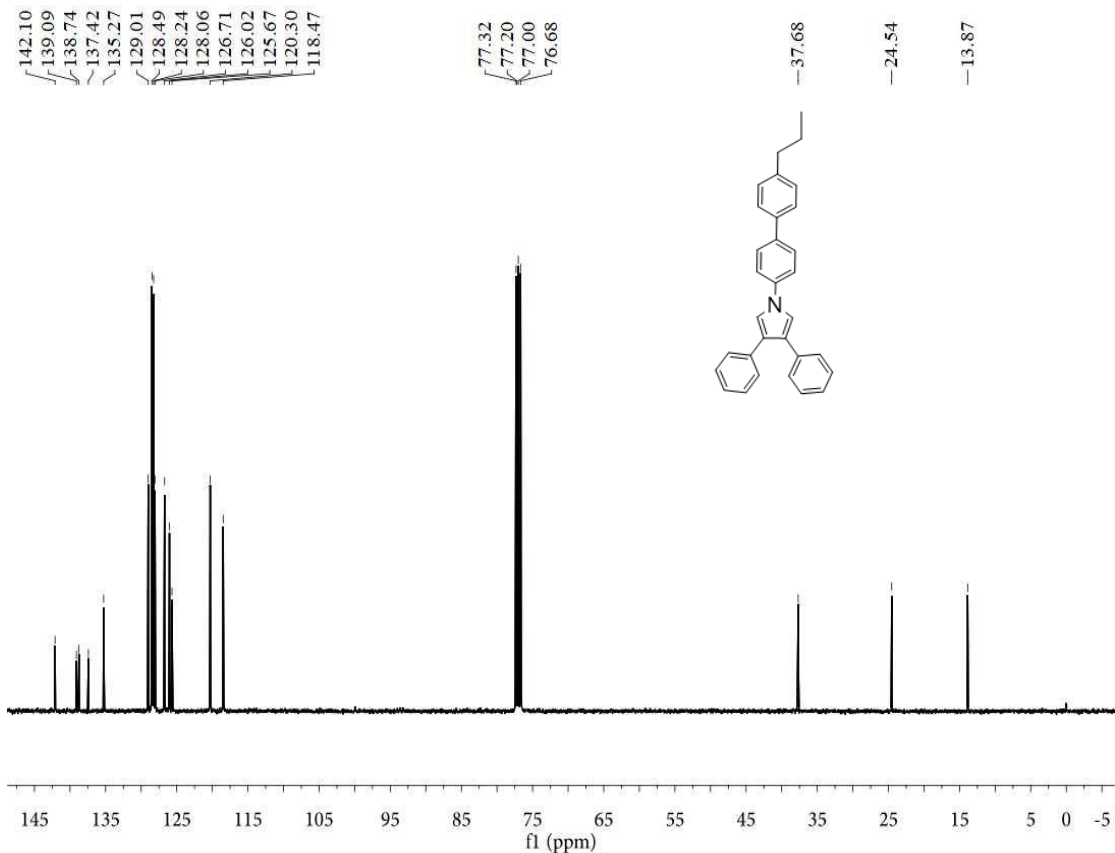


**Figure S19.** The  $^{13}\text{C}$  NMR of 1,3,4-C<sub>3</sub>H<sub>7</sub>. (CDCl<sub>3</sub>, 293 K, 400 M)

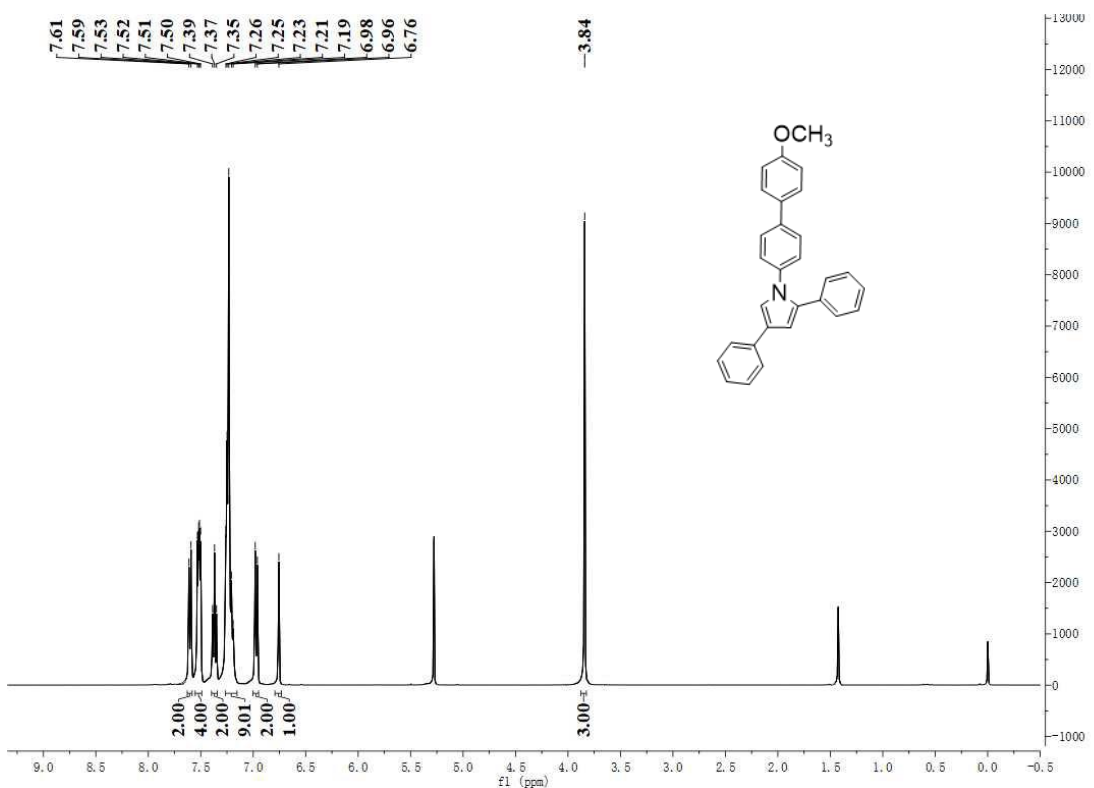


**Figure S20.** The  $^1\text{H}$  NMR of 1,2,4-OCH<sub>3</sub>. (CDCl<sub>3</sub>, 293 K, 400 M)

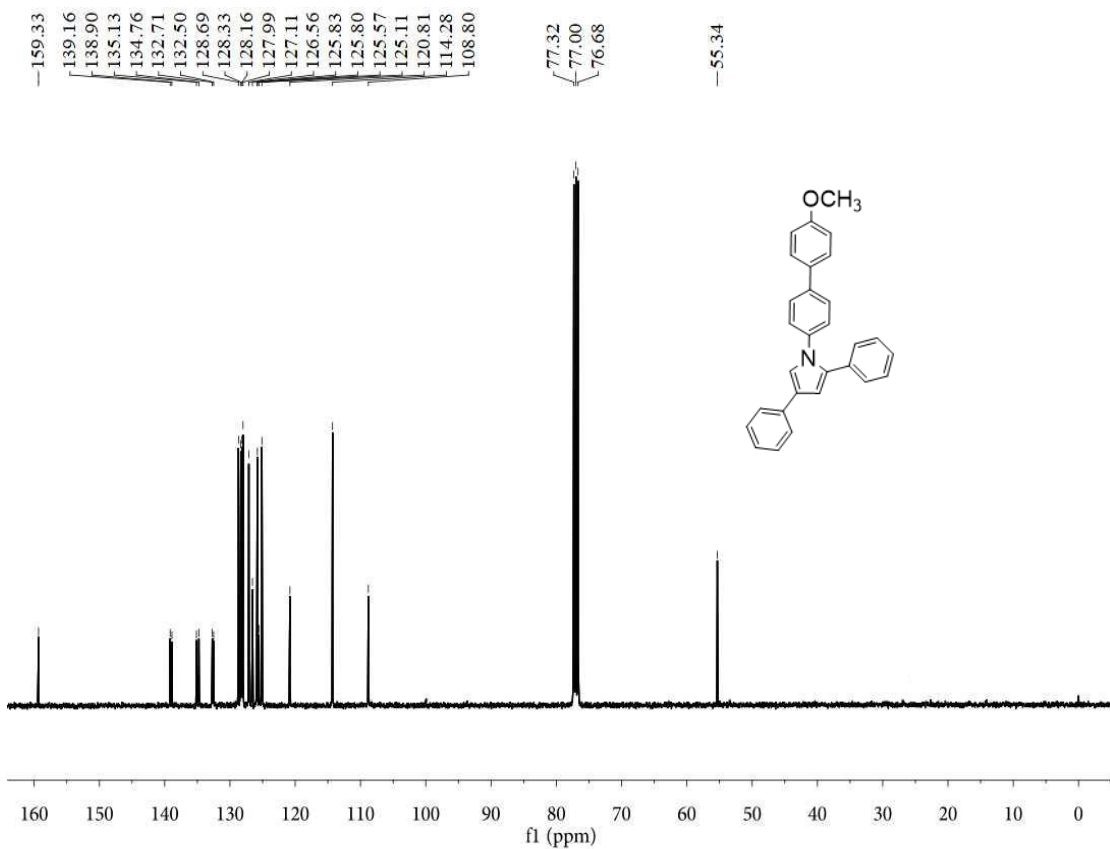


**Figure S21.** The  $^{13}\text{C}$  NMR of 1,2,4-OCH<sub>3</sub>. (CDCl<sub>3</sub>, 293 K, 400 M)

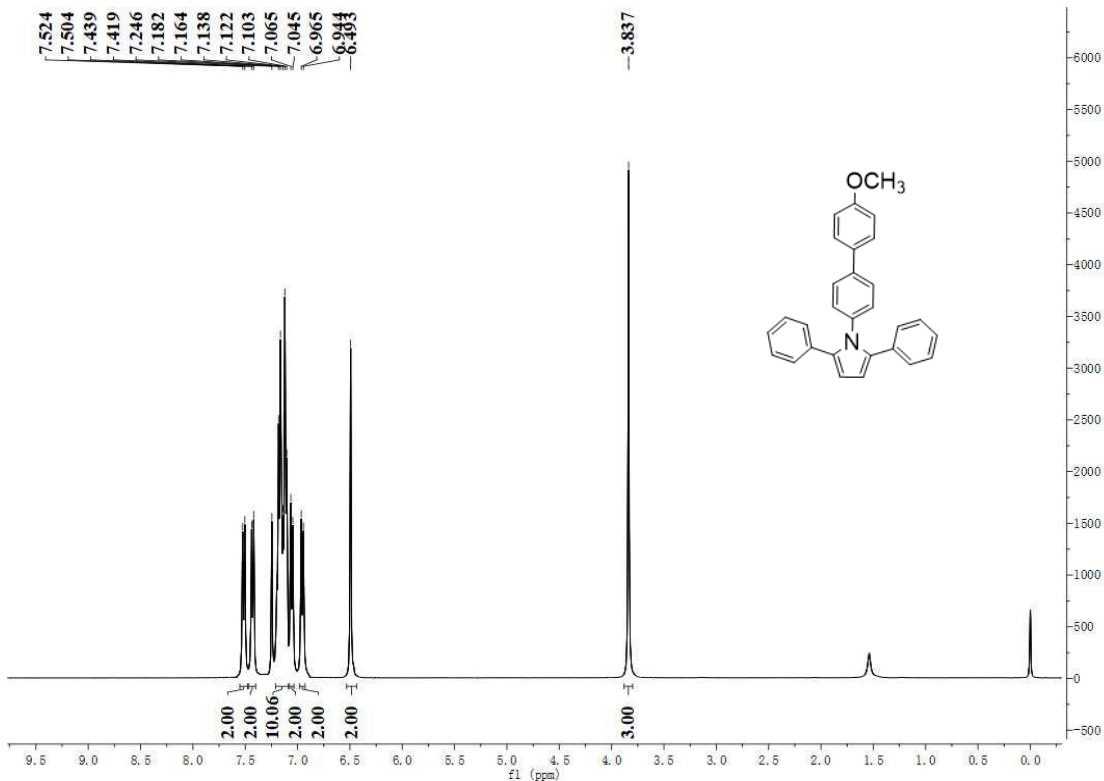


**Figure S22.** The <sup>1</sup>H NMR of 1,2,5-OCH<sub>3</sub>. (CDCl<sub>3</sub>, 293 K, 400 M)

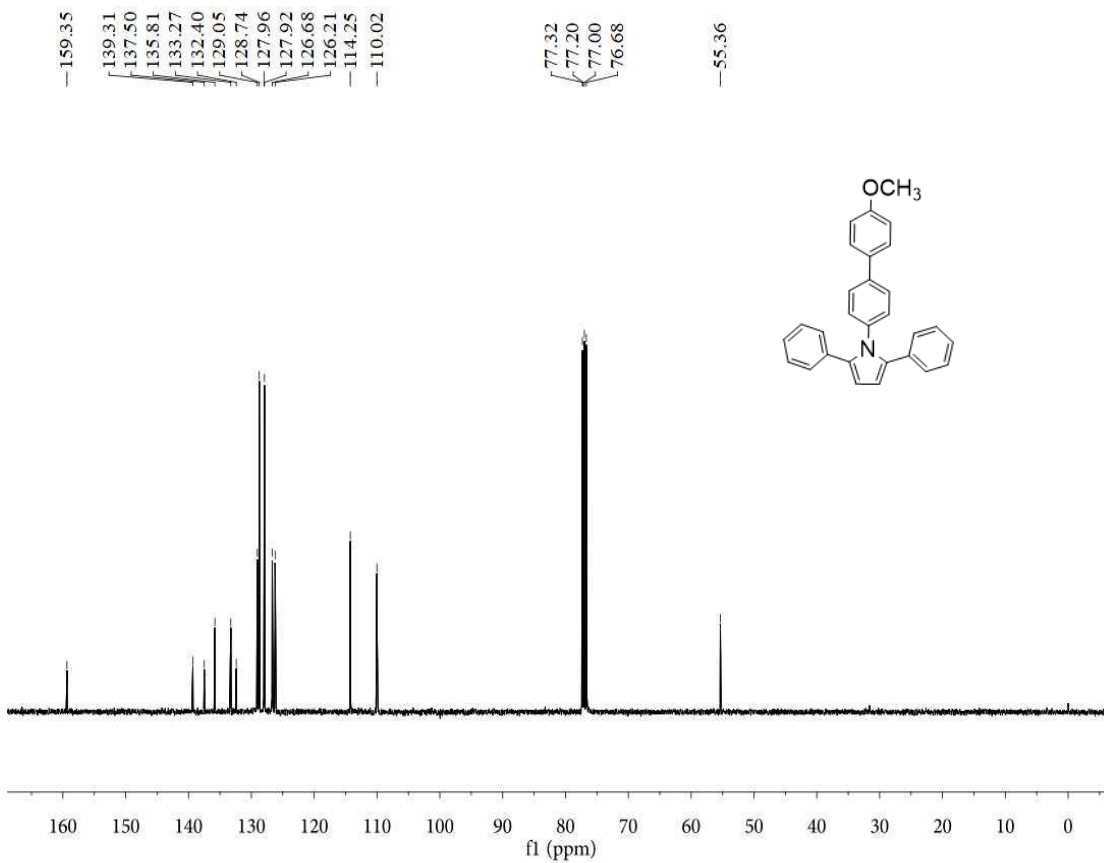


**Figure S23.** The <sup>13</sup>C NMR of 1,2,5-OCH<sub>3</sub>. (CDCl<sub>3</sub>, 293 K, 400 M)

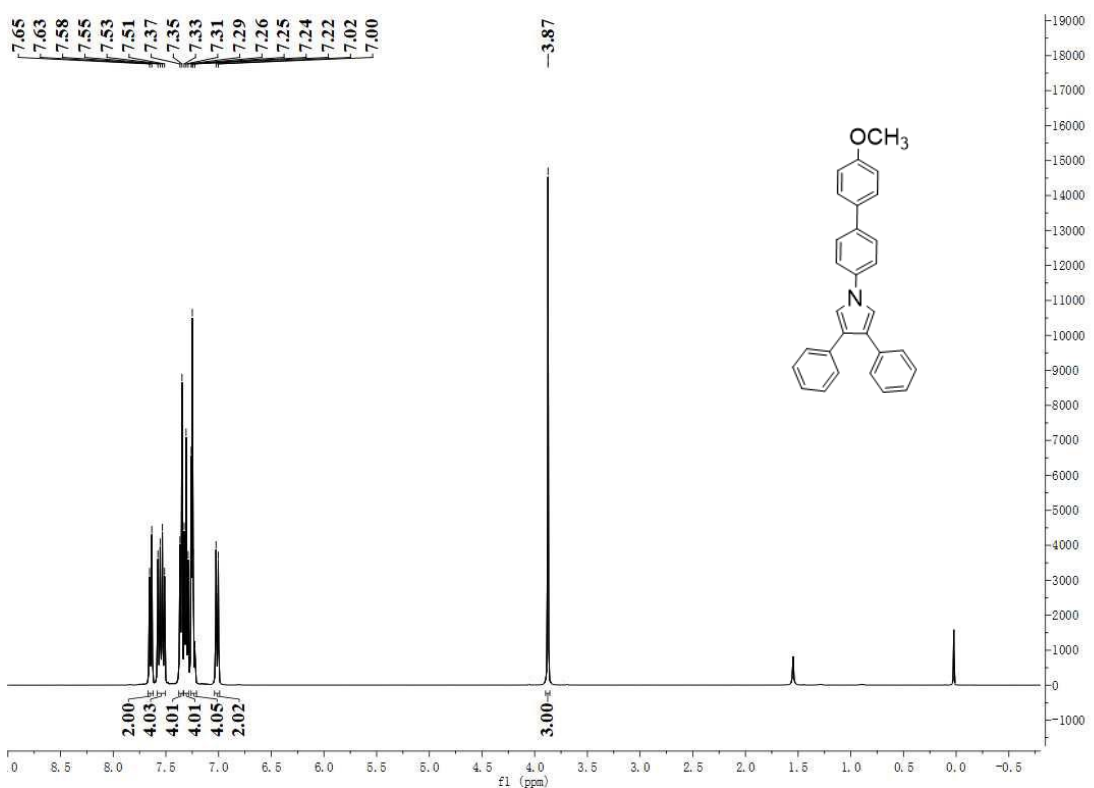


**Figure S24.** The  $^1\text{H}$  NMR of 1,3,4-OCH<sub>3</sub>. (CDCl<sub>3</sub>, 293 K, 400 M)

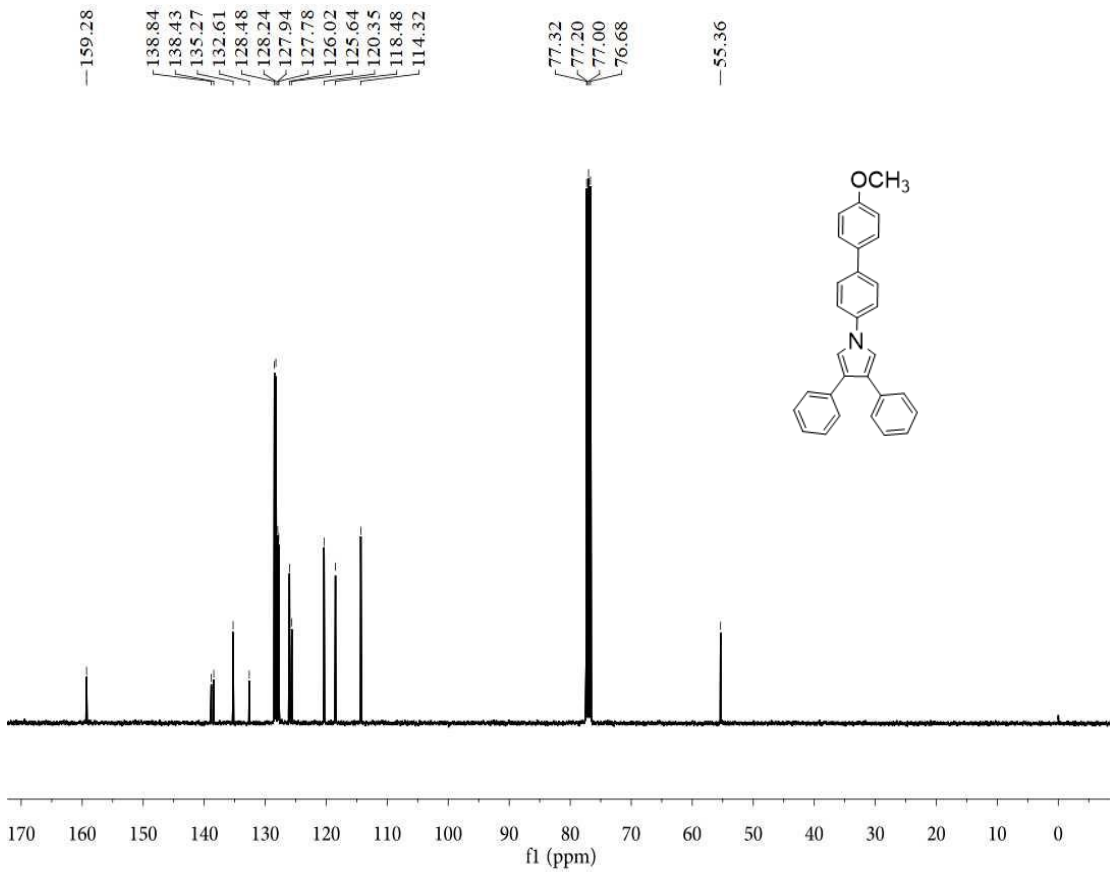


**Figure S25.** The  $^{13}\text{C}$  NMR of 1,3,4-OCH<sub>3</sub>. (CDCl<sub>3</sub>, 293 K, 400 M)

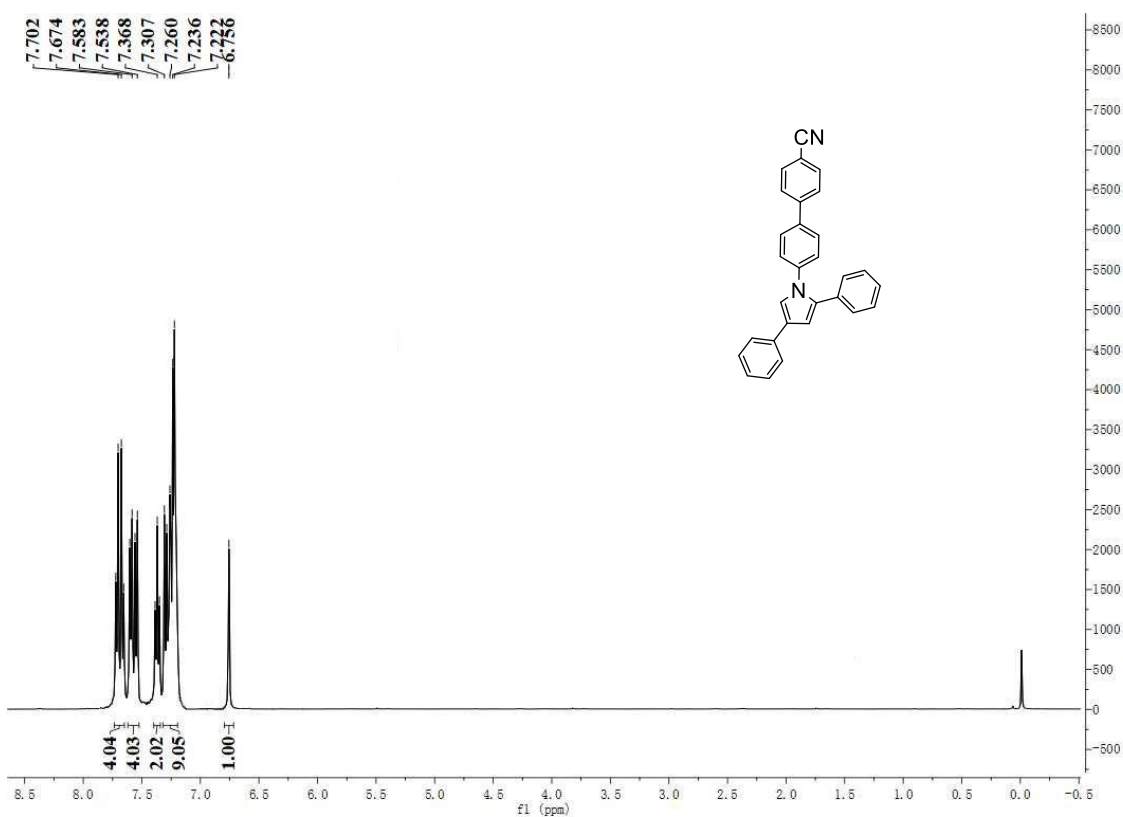


**Figure S26.** The  $^1\text{H}$  NMR of 1,2,4-CN. ( $\text{CDCl}_3$ , 293 K, 400 M)

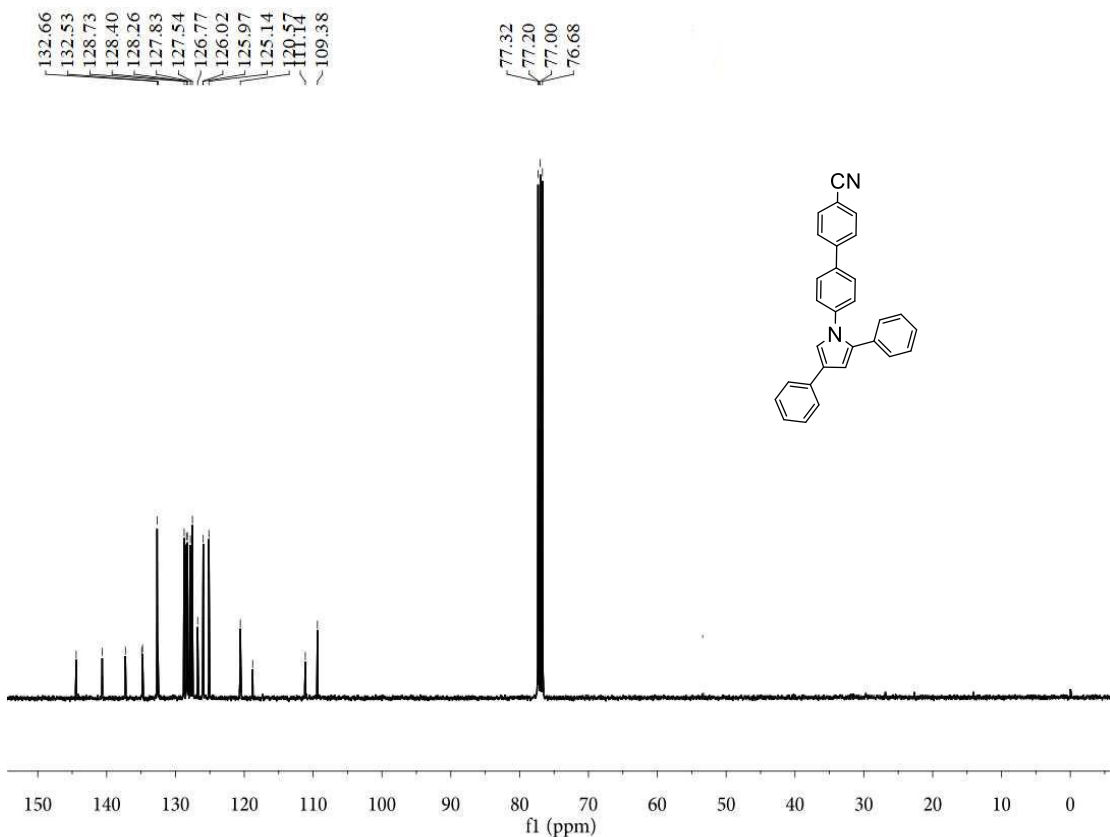


**Figure S27.** The  $^{13}\text{C}$  NMR of 1,2,4-CN. ( $\text{CDCl}_3$ , 293 K, 400 M)

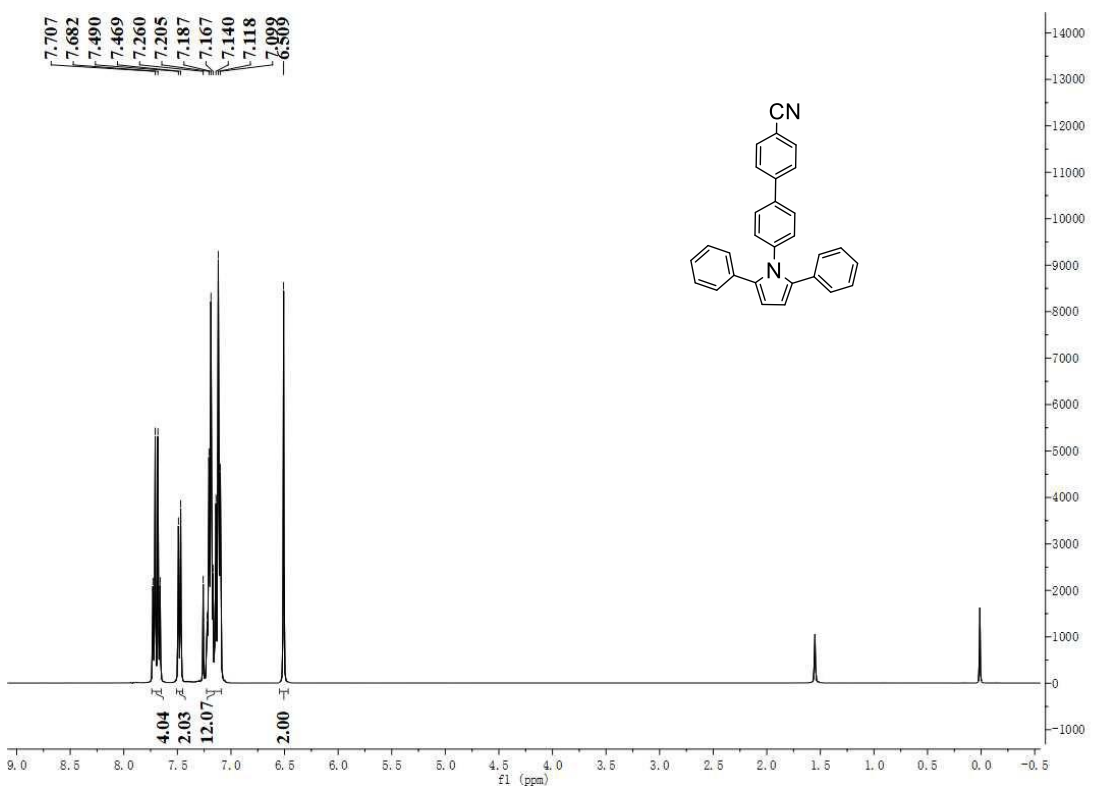


**Figure S28.** The  $^1\text{H}$  NMR of 1,2,5-CN. ( $\text{CDCl}_3$ , 293 K, 400 M)

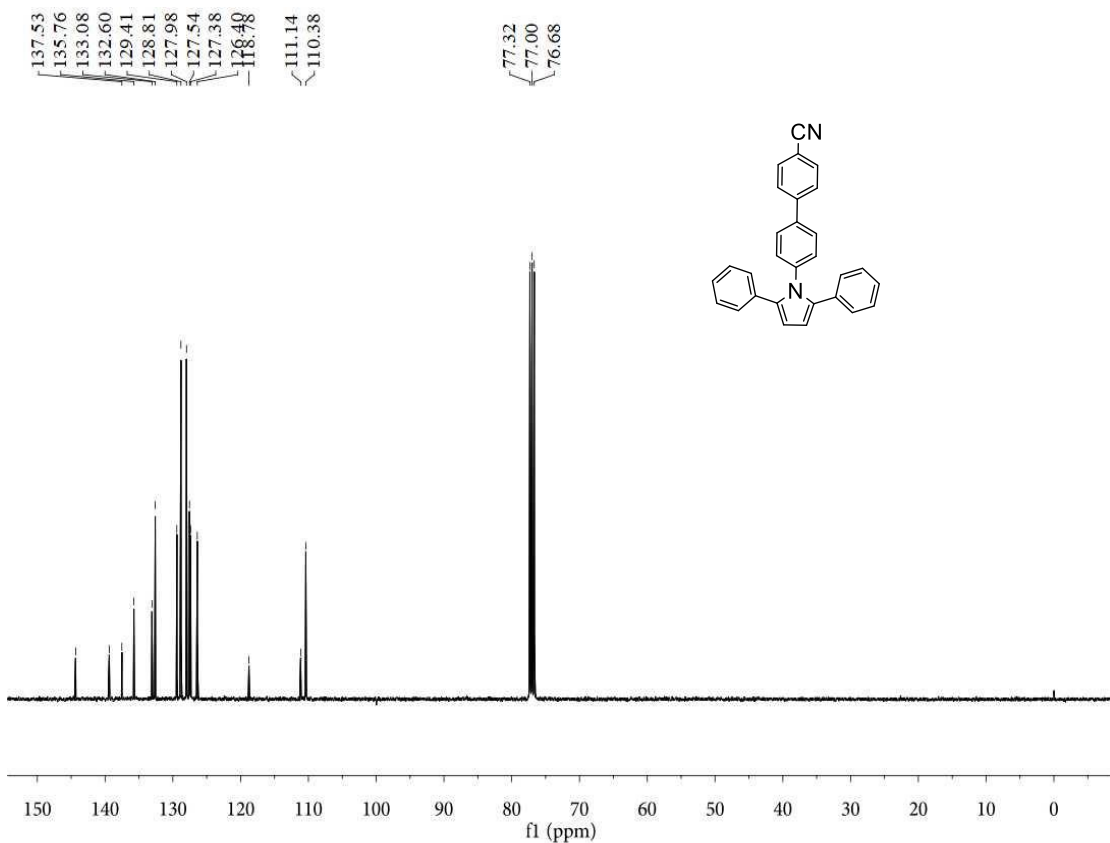


**Figure S29.** The  $^{13}\text{C}$  NMR of 1,2,5-CN. ( $\text{CDCl}_3$ , 293 K, 400 M)

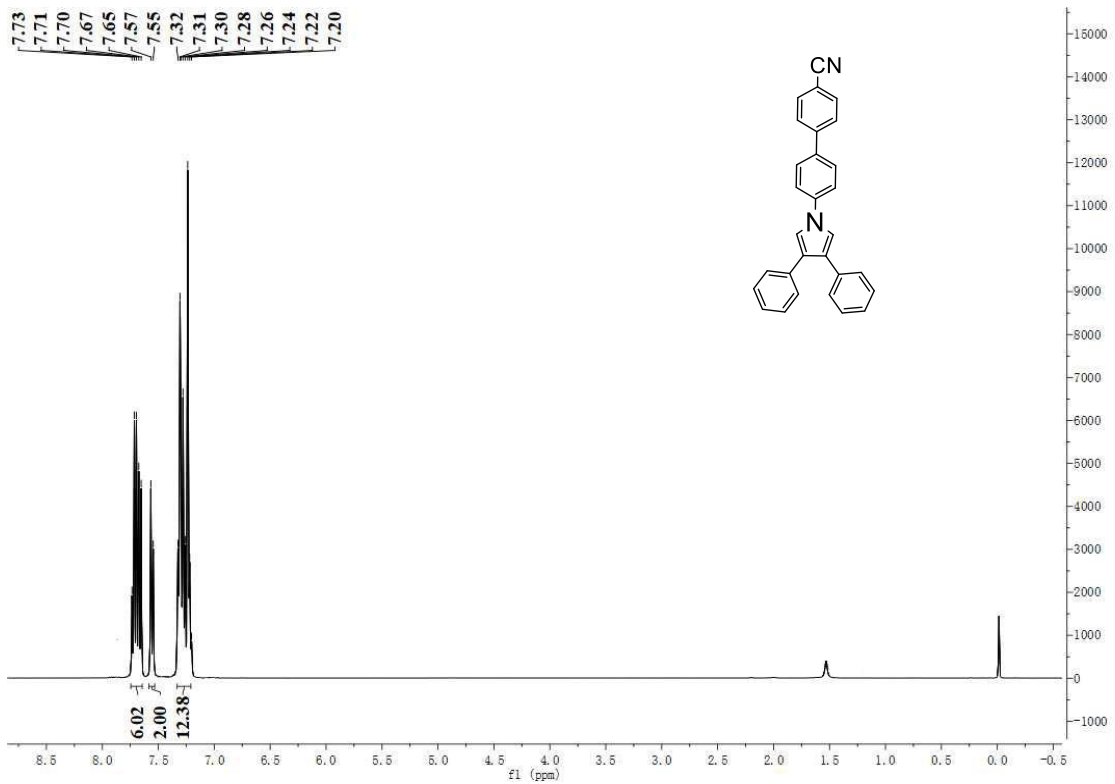


**Figure S30.** The  $^1\text{H}$  NMR of 1,3,4-CN. ( $\text{CDCl}_3$ , 293 K, 400 M)

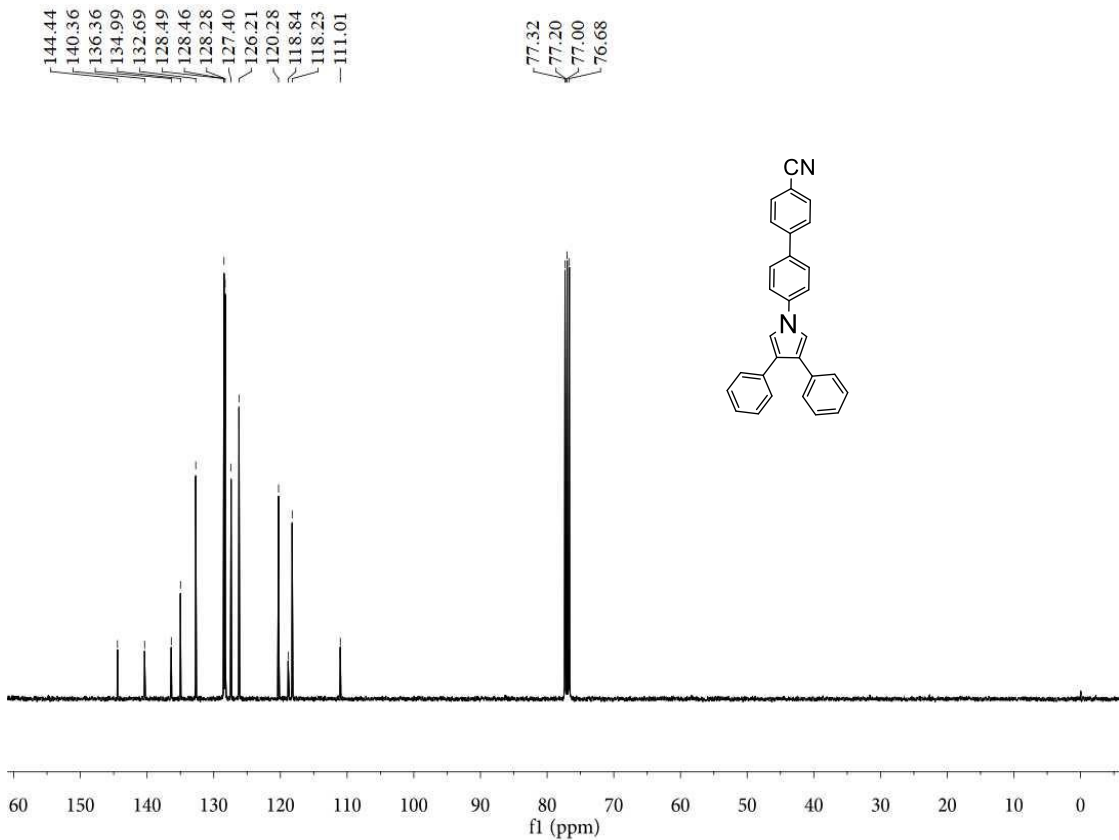


**Figure S31.** The  $^{13}\text{C}$  NMR of 1,3,4-CN. ( $\text{CDCl}_3$ , 293 K, 400 M)

**Table S3.** Crystal data and structure refinement for 1,2,4-OCH<sub>3</sub>.

Identification code	bwn18026
Empirical formula	C <sub>29</sub> H <sub>23</sub> NO
Formula weight	401.48
Temperature/K	153.15
Crystal system	monoclinic
Space group	C2/c
a/Å	31.660(6)
b/Å	5.9010(12)
c/Å	22.932(5)
α/°	90
β/°	100.11(3)
γ/°	90
Volume/Å <sup>3</sup>	4217.8(15)
Z	8
ρ <sub>calcg</sub> /cm <sup>3</sup>	1.265
μ/mm <sup>-1</sup>	0.076
F(000)	1696.0
Crystal size/mm <sup>3</sup>	0.21 × 0.12 × 0.1
Radiation	MoKα ( $\lambda = 0.71073$ )
2Θ range for data collection/°	2.614 to 54.94
Index ranges	-40 ≤ h ≤ 40, -7 ≤ k ≤ 7, -27 ≤ l ≤ 29
Reflections collected	14302
Independent reflections	4807 [R <sub>int</sub> = 0.0462, R <sub>sigma</sub> = 0.0463]
Data/restraints/parameters	4807/0/281
Goodness-of-fit on F <sup>2</sup>	1.267
Final R indexes [I>=2σ (I)]	R <sub>1</sub> = 0.0781, wR <sub>2</sub> = 0.2294
Final R indexes [all data]	R <sub>1</sub> = 0.0955, wR <sub>2</sub> = 0.2679
Largest diff. peak/hole / e Å <sup>-3</sup>	0.49/-0.43

**Table S4.** Crystal data and structure refinement for 1,3,4-OCH<sub>3</sub>.

Empirical formula	C <sub>29</sub> H <sub>23</sub> NO
Formula weight	401.48
Temperature/K	153.15
Crystal system	orthorhombic
Space group	Pca <sub>2</sub> <sub>1</sub>
a/Å	45.210(9)
b/Å	6.1483(12)
c/Å	7.4490(15)
α/°	90
β/°	90
γ/°	90
Volume/Å <sup>3</sup>	2070.5(7)
Z	4
ρ <sub>calc</sub> g/cm <sup>3</sup>	1.288
μ/mm <sup>-1</sup>	0.077
F(000)	848.0
Crystal size/mm <sup>3</sup>	0.24 × 0.23 × 0.02
Radiation	MoKα ( $\lambda = 0.71073$ )
2Θ range for data collection/°	6.55 to 52.64
Index ranges	-56 ≤ h ≤ 51, -7 ≤ k ≤ 7, -9 ≤ l ≤ 8
Reflections collected	11634
Independent reflections	3981 [R <sub>int</sub> = 0.0444, R <sub>sigma</sub> = 0.0457]
Data/restraints/parameters	3981/1/281
Goodness-of-fit on F <sup>2</sup>	1.150
Final R indexes [I>=2σ (I)]	R <sub>1</sub> = 0.0664, wR <sub>2</sub> = 0.1404
Final R indexes [all data]	R <sub>1</sub> = 0.0723, wR <sub>2</sub> = 0.1459
Largest diff. peak/hole / eÅ <sup>-3</sup>	0.20/-0.23
Flack parameter	0.3(10)

**Table S5.** Crystal data and structure refinement for 1,3,4-C<sub>3</sub>H<sub>7</sub>

Empirical formula	C <sub>31</sub> H <sub>27</sub> N
Formula weight	413.53
Temperature/K	153.15
Crystal system	monoclinic
Space group	Cc
a/Å	42.454(9)
b/Å	11.064(2)
c/Å	9.786(2)
α/°	90
β/°	94.49(3)
γ/°	90
Volume/Å <sup>3</sup>	4582.6(16)
Z	8
ρ <sub>calc</sub> g/cm <sup>3</sup>	1.199
μ/mm <sup>-1</sup>	0.069
F(000)	1760.0
Crystal size/mm <sup>3</sup>	0.13 × 0.12 × 0.02
Radiation	MoKα ( $\lambda = 0.71073$ )
2Θ range for data collection/°	3.85 to 49.998
Index ranges	-50 ≤ h ≤ 49, -13 ≤ k ≤ 13, -11 ≤ l ≤ 11
Reflections collected	12368
Independent reflections	7680 [R <sub>int</sub> = 0.0602, R <sub>sigma</sub> = 0.0978]
Data/restraints/parameters	7680/890/608
Goodness-of-fit on F <sup>2</sup>	1.103
Final R indexes [I>=2σ (I)]	R <sub>1</sub> = 0.1348, wR <sub>2</sub> = 0.2727
Final R indexes [all data]	R <sub>1</sub> = 0.1596, wR <sub>2</sub> = 0.2993
Largest diff. peak/hole / e Å <sup>-3</sup>	0.43/-0.41
Flack parameter	-4.4(10)

**Table S6.** Crystal data and structure refinement for 1,2,4-CN.

Empirical formula	C <sub>29</sub> H <sub>20</sub> N <sub>2</sub>
Formula weight	396.47
Temperature/K	153.15
Crystal system	orthorhombic
Space group	Pca2 <sub>1</sub>
a/Å	8.7745(18)
b/Å	11.508(2)
c/Å	20.298(4)
α/°	90
β/°	90
γ/°	90
Volume/Å <sup>3</sup>	2049.7(7)
Z	4
ρ <sub>calc</sub> g/cm <sup>3</sup>	1.285
μ/mm <sup>-1</sup>	0.075
F(000)	832.0
Crystal size/mm <sup>3</sup>	0.12 × 0.11 × 0.03
Radiation	MoKα ( $\lambda = 0.71073$ )
2Θ range for data collection/°	3.54 to 49.996
Index ranges	-10 ≤ h ≤ 10, -13 ≤ k ≤ 13, -23 ≤ l ≤ 24
Reflections collected	19342
Independent reflections	3574 [R <sub>int</sub> = 0.0920, R <sub>sigma</sub> = 0.0652]
Data/restraints/parameters	3574/1/280
Goodness-of-fit on F <sup>2</sup>	1.220
Final R indexes [I>=2σ (I)]	R <sub>1</sub> = 0.0772, wR <sub>2</sub> = 0.1932
Final R indexes [all data]	R <sub>1</sub> = 0.0919, wR <sub>2</sub> = 0.2209
Largest diff. peak/hole / e Å <sup>-3</sup>	0.44/-0.44
Flack parameter	-0.9(10)

**Table S7.** Crystal data and structure refinement for 1,2,5-CN.

Empirical formula	C <sub>32</sub> H <sub>27</sub> N <sub>3</sub> O
Formula weight	469.56
Temperature/K	153.15
Crystal system	monoclinic
Space group	P2 <sub>1</sub> /c
a/Å	23.528(5)
b/Å	6.0582(12)
c/Å	17.914(4)
α/°	90
β/°	93.56(3)
γ/°	90
Volume/Å <sup>3</sup>	2548.5(9)
Z	4
ρ <sub>calc</sub> g/cm <sup>3</sup>	1.224
μ/mm <sup>-1</sup>	0.075
F(000)	992.0
Crystal size/mm <sup>3</sup>	0.13 × 0.05 × 0.02
Radiation	MoKα ( $\lambda = 0.71073$ )
2Θ range for data collection/°	1.734 to 49.998
Index ranges	-27 ≤ h ≤ 27, -7 ≤ k ≤ 7, -20 ≤ l ≤ 21
Reflections collected	23821
Independent reflections	4461 [R <sub>int</sub> = 0.1295, R <sub>sigma</sub> = 0.0810]
Data/restraints/parameters	4461/468/338
Goodness-of-fit on F <sup>2</sup>	2.771
Final R indexes [I>=2σ (I)]	R <sub>1</sub> = 0.2562, wR <sub>2</sub> = 0.6218
Final R indexes [all data]	R <sub>1</sub> = 0.2738, wR <sub>2</sub> = 0.6310
Largest diff. peak/hole / e Å <sup>-3</sup>	0.93/-0.73

**Table S8.** Crystal data and structure refinement for 1,3,4-CN

Identification code	<b>1,3,4-CN</b>
Empirical formula	C <sub>29</sub> H <sub>20</sub> N <sub>2</sub>
Formula weight	396.47
Temperature/K	153.15
Crystal system	triclinic
Space group	P-1
a/Å	8.4662(17)
b/Å	15.145(3)
c/Å	17.692(4)
α/°	106.62(3)
β/°	95.32(3)
γ/°	91.57(3)
Volume/Å <sup>3</sup>	2160.8(8)
Z	4
ρ <sub>calcg</sub> /cm <sup>3</sup>	1.219
μ/mm <sup>-1</sup>	0.071
F(000)	832.0
Crystal size/mm <sup>3</sup>	0.21 × 0.03 × 0.02
Radiation	MoKα ( $\lambda = 0.71073$ )
2Θ range for data collection/°	2.416 to 49.996
Index ranges	-8 ≤ h ≤ 10, -18 ≤ k ≤ 18, -21 ≤ l ≤ 20
Reflections collected	17446
Independent reflections	7523 [ $R_{\text{int}} = 0.1042$ , $R_{\text{sigma}} = 0.1320$ ]
Data/restraints/parameters	7523/0/559
Goodness-of-fit on F <sup>2</sup>	1.239
Final R indexes [I>=2σ (I)]	$R_1 = 0.1627$ , $wR_2 = 0.3918$
Final R indexes [all data]	$R_1 = 0.2100$ , $wR_2 = 0.4353$
Largest diff. peak/hole / e Å <sup>-3</sup>	0.44/-0.46